

WL-TR-96-4081

Durability of Adhesively Bonded  
Aluminum and Titanium Performance for  
Non-Chemical Surface Treatments



Kristy L. Wolfe, Susan R. Harp and  
John G. Dillard

Department of Chemistry  
Virginia Polytechnic Inst. & State University  
301 Burrus Hall  
Blacksburg, VA 24061-0212

February 1996

FINAL REPORT FOR 4/01/93-12/31/95

APPROVED FOR PUBLIC RELEASE; DISTRIBUTION IS UNLIMITED

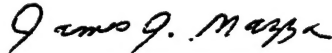
MATERIALS DIRECTORATE  
WRIGHT LABORATORY  
AIR FORCE MATERIEL COMMAND  
WRIGHT PATTERSON AFB OH 45433-7734

19990713 002

## NOTICE

WHEN GOVERNMENT DRAWINGS, SPECIFICATIONS, OR OTHER DATA ARE USED FOR ANY PURPOSE OTHER THAN IN CONNECTION WITH A DEFINITELY GOVERNMENT-RELATED PROCUREMENT, THE UNITED STATES GOVERNMENT INCURS NO RESPONSIBILITY OR ANY OBLIGATION WHATSOEVER. THE FACT THAT THE GOVERNMENT MAY HAVE FORMULATED OR IN ANY WAY SUPPLIED THE SAID DRAWINGS, SPECIFICATIONS, OR OTHER DATA, IS NOT TO BE REGARDED BY IMPLICATION, OR OTHERWISE IN ANY MANNER CONSTRUED, AS LICENSING THE HOLDER, OR ANY OTHER PERSON OR CORPORATION; OR AS CONVEYING ANY RIGHTS OR PERMISSION TO MANUFACTURE, USE, OR SELL ANY PATENTED INVENTION THAT MAY IN ANY WAY BE RELATED THERETO.

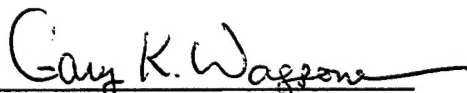
This technical report has been reviewed and is approved for publication.



JAMES J. MAZZA  
Project Engineer  
Materials Integrity Branch



MICHAEL F. HITCHCOCK  
Chief  
Materials Integrity Branch



GARY K. WAGGONER  
Chief  
Systems Support Division

IF YOUR ADDRESS HAS CHANGED, IF YOU WISH TO BE REMOVED FROM OUR MAILING LIST, OR IF THE ADDRESSEE IS NOT LONGER EMPLOYED BY YOUR ORGANIZATION PLEASE NOTIFY AFRL/MLS, 2179 TWELFTH ST. ROOM 122, WRIGHT-PATTERSON AFB, OH 45433-7718 TO HELP MAINTAIN A CURRENT MAILING LIST.

Copies of this report should not be returned unless return is required by security considerations, contractual obligations, or notice on a specific document.

# REPORT DOCUMENTATION PAGE

Form Approved  
OMB No. 0704-0188

Public reporting burden for this collection of information is estimated to average 1 hour per response, including the time for reviewing instructions, searching existing data sources, gathering and maintaining the data needed, and completing and reviewing the collection of information. Send comments regarding this burden estimate or any other aspect of this collection of information, including suggestions for reducing this burden, to Washington Headquarters Services, Directorate for Information Operations and Reports, 1215 Jefferson Davis Highway, Suite 1204, Arlington, VA 22202-4302, and to the Office of Management and Budget, Paperwork Reduction Project (0704-0188), Washington, DC 20503.

1. AGENCY USE ONLY (Leave blank)		2. REPORT DATE Feb. 96	3. REPORT TYPE AND DATES COVERED Final Apr. 1, 1993 - Dec. 31, 1995	
4. TITLE AND SUBTITLE Durability of Adhesively Bonded Aluminum and Titanium Performance for Non-Chemical Surface Treatments			5. FUNDING NUMBERS C F33615-93-C-5321 PE 62102F PR 2418 TA 04 WV FM	
6. AUTHOR(S) Kristy L. Wolfe, Susan R. Harp, and John G. Dillard				
7. PERFORMING ORGANIZATION NAME(S) AND ADDRESS(ES) Department of Chemistry Virginia Polytechnic Institute and State University 301 Burrus Hall Blacksburg, VA 24061-0212			8. PERFORMING ORGANIZATION REPORT NUMBER	
9. SPONSORING / MONITORING AGENCY NAME(S) AND ADDRESS(ES) Materials Directorate Wright Laboratory Air Force Materiel Command Wright - Patterson AFB, OH POC: James Mazza (513) 225-7778 45433-7734			10. SPONSORING / MONITORING AGENCY REPORT NUMBER WL-TR-96-4081	
11. SUPPLEMENTARY NOTES				
12a. DISTRIBUTION / AVAILABILITY STATEMENT  Approved for public release; distribution is unlimited.			12b. DISTRIBUTION CODE	
13. ABSTRACT (Maximum 200 words)  The durability of plasma-sprayed metals bonded with a polyimide or epoxy adhesive was studied. Metal adherend surfaces were prepared for adhesive bonding by plasma-spraying inorganic and polymeric powders on aluminum and titanium. The plasma-sprayed materials included Al <sub>2</sub> O <sub>3</sub> , AlPO <sub>4</sub> , MgO, and SiO <sub>2</sub> on aluminum; TiO, TiSi <sub>2</sub> , MgO, and SiO <sub>2</sub> on titanium; and polyester, epoxy, bismaleimide, and polyimide on aluminum and titanium. Durability studies used samples prepared in a wedge-type durability geometry. Durability was investigated via an environmental cycle that included exposure to the conditions: low temperature -20°C (-5°F); (160°C; 320°F) in vacuum (130 torr, 0.2 atm); and room temperature. The crack growth rate for thin coatings (25 µm) of Al <sub>2</sub> O <sub>3</sub> , AlPO <sub>4</sub> , SiO <sub>2</sub> , and MgO plasma-sprayed on aluminum was equivalent to that for phosphoric acid anodized aluminum. The performance for titanium samples prepared with a 25 µm-thick TiO <sub>2</sub> , TiSi <sub>2</sub> and SiO <sub>2</sub> plasma-sprayed coatings was equivalent to that for a Turco 5578-prepared titanium surface. The systems exhibiting durability comparable to that for adherends treated using the standard solution methods, included aluminum or titanium coated with bismaleimide/cyanate ester (BMI-CE) or a bismaleimide-LaRC TPI-1500 mixture bonded with an epoxy or a polyimide adhesive.				
14. SUBJECT TERMS Plasma Spray, Inorganic Coatings, Polymer Coatings, Adhesive Bonding, Durability, Environmental Cycle, Surface Analysis			15. NUMBER OF PAGES 80	
			16. PRICE CODE	
17. SECURITY CLASSIFICATION OF REPORT Unclassified	18. SECURITY CLASSIFICATION OF THIS PAGE Unclassified	19. SECURITY CLASSIFICATION OF ABSTRACT Unclassified	20. LIMITATION OF ABSTRACT SAR	

## Table of Contents

	List of Figures -----	iii
	List of Tables -----	v
1.	Summary-----	1
2.	Introduction -----	5
3.	Experimental Section-----	9
4.	Plasma-Sprayed Adherends - Surface Characterizatin of Aluminum and Titanium-----	18
5.	Plasma-Sprayed Adherends - Durability of Adherends Coated with Inorganic Materials -----	38
6.	Plasma-Sprayed Adherends - Durability of Adherends Coated with Polymeric Materials -----	50
7.	Durability Investigation of Butt-Torsion Specimens -----	59
8.	Summary and Conclusions -----	72
9.	References-----	74



## List of Figures

<b>Figure 1.</b>	Bonding rack for the preparation of butt-torsion specimens-----	13
<b>Figure 2.</b>	Durability testing apparatus for butt-torsion specimens -----	16
<b>Figure 3.</b>	Scanning electron photomicrograph of polyester powder plasma-sprayed on titanium -----	19
<b>Figure 4.</b>	Scanning electron photomicrograph of Bismaleimide-LaRC-TPI powder mixture plasma-sprayed on titanium-----	20
<b>Figure 5.</b>	Scanning electron photomicrograph of $\text{Al}_2\text{O}_3$ powder plasma-sprayed on aluminum-----	21
<b>Figure 6.</b>	Scanning electron photomicrograph of $\text{AlPO}_4$ powder plasma-sprayed on aluminum-----	22
<b>Figure 7.</b>	Scanning electron photomicrograph of $\text{TiO}_2$ powder plasma-sprayed on titanium -----	23
<b>Figure 8.</b>	Scanning electron photomicrograph of $\text{MgO}$ powder plasma-sprayed on aluminum-----	24
<b>Figure 9.</b>	Scanning electron photomicrograph of $\text{SiO}_2$ powder plasma-sprayed on aluminum-----	25
<b>Figure 10.</b>	Scanning electron photomicrograph of $\text{TiSi}_2$ powder plasma-sprayed on titanium -----	26
<b>Figure 11.</b>	Carbon 1s x-ray photoelectron spectra for: a) epoxy polymer powder; b) epoxy polymer powder plasma-sprayed on titanium -----	29
<b>Figure 12.</b>	Carbon 1s x-ray photoelectron spectra for: a) polyester polymer powder; b) polyester polymer powder plasma-sprayed on titanium -----	30
<b>Figure 13.</b>	Titanium 2p x-ray photoelectron spectra for: a) $\text{TiSi}_2$ powder; b) $\text{TiSi}_2$ powder plasma-sprayed on titanium -----	35

<b>Figure 14.</b> Silicon 2p x-ray photoelectron spectra for: a) $\text{TiSi}_2$ powder; b) $\text{TiSi}_2$ powder plasma-sprayed on titanium -----	36
<b>Figure 15.</b> Crack Length Results for Plasma-Sprayed Aluminum Adherends Bonded with FM-36 Polyimide Adhesive; Time: 0 to 172 hrs. Total environmental exposure duration 3500 hrs. Crack lengths at 172 hrs. equal to lengths at 3500 hrs. -----	39
<b>Figure 16.</b> Crack Length Results for Plasma-Sprayed Titanium Adherends Bonded with FM-36 Polyimide Adhesive; Time: 0 to 172 hrs. Total environmental exposure duration 3500 hrs. Crack lengths at 172 hrs. equal to lengths at 3500 hrs. -----	40
<b>Figure 17.</b> Crack Length Results for Plasma-Sprayed Aluminum Adherends Bonded with FM-36 Polyimide Adhesive; Crack length during the first environmental cycle -----	41
<b>Figure 18.</b> Crack Length Results for Plasma-Sprayed Titanium Adherends Bonded with FM-36 Polyimide Adhesive; Crack length during the first environmental cycle -----	42
<b>Figure 19.</b> Wedge Specimen Durability: Crack length vs. time of environmental exposure for plasma-sprayed aluminum and titanium bonded with an epoxy adhesive (AF-191)-----	51
<b>Figure 20.</b> Wedge Specimen Durability: Crack length vs. time of environmental exposure for plasma-sprayed aluminum and titanium bonded with a polyimide adhesive (FM-36)-----	52

## List of Tables

<b>Table 1.</b>	Inorganic Powders and Suppliers-----	10
<b>Table 2.</b>	Polymer Powders and Suppliers-----	10
<b>Table 3.</b>	XPS Characterization Results for Organic-Polymer Plasma-Sprayed Materials-----	28
<b>Table 4.</b>	XPS Results for Inorganic Powders-----	31
<b>Table 5.</b>	XPS Results for Inorganic Plasma-Sprayed Coatings-----	32
<b>Table 6.</b>	Allocation of Oxygen Containing Constituents: Plasma-Sprayed Coatings-----	33
<b>Table 7.</b>	Failure Processes for Plasma Sprayed Adherends: Aluminum Bonded with FM-36 Polyimide Adhesive-----	45
<b>Table 8.</b>	Failure Processes for Plasma Sprayed Adherends: Titanium Bonded with FM-36 Polyimide Adhesive-----	45
<b>Table 9.</b>	Surface Analysis Results for $\text{Al}_2\text{O}_3/\text{Al}$ Plasma-Sprayed Specimens and Failure Surfaces-----	46
<b>Table 10.</b>	Surface Analysis Results for $\text{AlPO}_4/\text{Al}$ Plasma-Sprayed Specimens and Failure Surfaces-----	47
<b>Table 11.</b>	Initial and Arrest Crack Length Values and Failure Modes for Plasma-Sprayed Aluminum Adherends-----	53
<b>Table 12.</b>	Initial and Arrest Crack Length Values and Failure Modes for Plasma-Sprayed Titanium-6Al-4V Adherends-----	54
<b>Table 13.</b>	Butt-torsion Test Results - Initial Determination of Failure Torque-----	59
<b>Table 14.</b>	Anodization Failure Results-----	61
<b>Table 15.</b>	Vinyl Phosphonic Acid Failure Results-----	62
<b>Table 16.</b>	P2 Etch Failure Results-----	63
<b>Table 17.</b>	Aluminum Adherend: Plasma-sprayed Butt-torsion Samples-----	68
<b>Table 18.</b>	Titanium Adherend: Plasma-sprayed Butt-torsion Samples-----	70

## 1. Summary

### 1.1 Plasma-Sprayed Adherends - Surface Characterization of Aluminum and Titanium

The morphological and surface chemical properties of plasma-sprayed coatings on metals were investigated using surface characterization techniques. Organic-polymeric and inorganic powders were plasma-sprayed on aluminum and titanium. Organic-polymeric coatings were prepared using epoxy, polyester, polyimide, and cyanate ester components. Inorganic coatings were obtained by plasma-spraying  $\text{Al}_2\text{O}_3$ ,  $\text{AlPO}_4$ ,  $\text{MgO}$ , and  $\text{SiO}_2$  on aluminum, and  $\text{TiO}_2$ ,  $\text{TiSi}_2$ ,  $\text{MgO}$ , and  $\text{SiO}_2$  on titanium. The organic-polymeric coatings were prepared at one thickness (75-125  $\mu\text{m}$ ; 0.003"-0.005") while the inorganic coatings were sprayed to obtain two different thicknesses (25 and 150  $\mu\text{m}$ ; 0.001"-0.006"). SEM photographs reveal various morphological differences in the sprayed specimens. The surface morphology ranged from smooth to nodular among the plasma sprayed specimens. Surface chemical analysis of the plasma-sprayed coatings indicated that little or no chemical degradation of the components occurred as a result of plasma-spraying. However, plasma-sprayed  $\text{TiSi}_2$  appeared to be a mixture of silica and a titanium silicate.

### 1.2 Plasma-Sprayed Adherends - Durability of Adherends Coated with Inorganic Materials

The durability of plasma-sprayed metals bonded with a polyimide adhesive was studied. Metal adherend surfaces were prepared for adhesive bonding by plasma-spraying inorganic powders on aluminum and titanium. The plasma-sprayed materials included  $\text{Al}_2\text{O}_3$ ,  $\text{AlPO}_4$ ,  $\text{MgO}$ , and  $\text{SiO}_2$  on aluminum, and  $\text{TiO}_2$ ,  $\text{TiSi}_2$ ,  $\text{MgO}$ , and  $\text{SiO}_2$  on titanium. Durability studies of samples prepared in a wedge-type geometry were carried out. Bonded specimens were maintained in an environmental cycle that included exposure to the conditions; low temperature,  $-20^\circ\text{C}$  ( $-5^\circ\text{F}$ ); relative humidity at elevated temperature, 70% RH at  $66^\circ\text{C}$  ( $151^\circ\text{F}$ ); elevated temperature ( $160^\circ\text{C}$ ;  $320^\circ\text{F}$ ) in air, high temperature ( $160^\circ\text{C}$ ;  $320^\circ\text{F}$ ) in vacuum (130 torr, 0.2 atm.), and room

temperature. Crack growth rate and mode of failure were determined. The results of the durability tests indicate that thin coatings (25  $\mu\text{m}$ ; 0.001") of plasma-sprayed materials perform better than thicker (150  $\mu\text{m}$ ; 0.006") coatings. The crack growth rate for thin coatings (25  $\mu\text{m}$ ; 0.001") of  $\text{Al}_2\text{O}_3$ ,  $\text{AlPO}_4$ ,  $\text{SiO}_2$ , and  $\text{MgO}$  plasma-sprayed on aluminum was equivalent to that for phosphoric acid anodized aluminum. Similarly, the durability performance for titanium samples prepared with a 25  $\mu\text{m}$ -thick (0.001")  $\text{TiO}_2$ ,  $\text{TiSi}_2$ , and  $\text{SiO}_2$  plasma-sprayed coatings was equivalent to that for a Turco-prepared titanium surface. Although the evaluation of durability as a function of surface chemistry was an objective of the study, it was not possible to evaluate the effect, since most failures occurred within the adhesive (cohesive failure) during the environmental tests. That failure occurred in the adhesive indicates that the coating-adherend and the coating-adhesive interactions are sufficiently robust to prevent interfacial failure under the experimental conditions investigated.

### 1.3 Plasma-Sprayed Adherends - Durability of Adherends Coated with Polymeric Materials

The durability of aluminum and titanium adherends that had been plasma-sprayed with polymeric coatings and bonded with epoxy and a polyimide adherends were investigated. Organic-polymeric coatings were plasma-sprayed using epoxy, polyester, polyimide, and cyanate ester components. Durability was investigated using a wedge-type specimen by exposing the specimens to an environmental cycle that included low temperature, high relative humidity at elevated temperature, high temperature at atmospheric pressure in air, high temperature in a vacuum, and room temperature. The systems exhibiting durability comparable to that for adherends treated using standard solution methods, included aluminum or titanium coated with a bis-maleimide/cyanate ester (BMI-CE) or a bis-maleimide-LaRC TPI-1500 mixture and bonded with an epoxy or a polyimide adhesive. As a general observation, failure during exposure to the environmental cycle occurred in the adhesive (cohesive failure).

#### 1.4 Durability Investigation of Butt-Torsion Specimens

Plasma-sprayed aluminum and titanium adherends were bonded in a butt-torsion geometry using an epoxy and a polyimide adhesive. Specimens were stressed at 20% of the ultimate failure load and were maintained for up to 17,000 hrs. in an environmental cycle that included exposure to the conditions; low temperature, -20°C (-5°F); relative humidity at elevated temperature, 70% RH at 66°C; elevated temperature (160°C; 320°F) in air, high temperature (160°C; 320°F) in vacuum (130 torr, 0.2 atm.), and room temperature. Time to failure was determined and was used as a measure of specimen durability. Acceptable performance was identified for the situation where not more than half of the specimens failed during the tests, and where cohesive failure was noted. Coating (thickness-  $\mu\text{m}$ )/adherend/adhesive component combinations for which acceptable performance was demonstrated during the tests (up to about 17,000 hrs) included:

##### Aluminum adherends

25- $\text{Al}_2\text{O}_3$ /Al/epoxy

25- $\text{SiO}_2$ /Al/epoxy

25- $\text{Al}_2\text{O}_3$ /Al/polyimide

25- $\text{SiO}_2$ /Al/polyimide

##### Titanium adherends

50- $\text{SiO}_2$ /Ti/epoxy

150- $\text{MgO}$ /Ti/epoxy

25- $\text{TiSi}_2$ /Ti/epoxy

25- $\text{TiO}_2$ /Ti/polyimide

150- $\text{TiO}_2$ /Ti/polyimide

25- $\text{TiSi}_2$ /Ti/polyimide

25- $\text{SiO}_2$ /Ti/polyimide

TPI/Ti/polyimide

CE/Ti/polyimide

#### 1.5 Summary recommendations

The overall findings in this work indicate that thin coatings exhibit good performance as measured either by crack growth for wedge specimens or via time to failure for samples prepared using a butt-torsion geometry. The chemical systems that

show acceptable performance as plasma-sprayed coatings include  $\text{Al}_2\text{O}_3/\text{Al}$ ,  $\text{SiO}_2/\text{Al}$ ,  $\text{TiO}_2/\text{Ti}$ ,  $\text{TiSi}_2/\text{Ti}$ ,  $\text{SiO}_2/\text{Ti}$ ,  $\text{MgO}/\text{Ti}$ , and  $\text{TPI}/\text{Ti}$  and marginal performance for  $\text{CE}/\text{Ti}/\text{polyimide}$ . It should be recognized that spraying was only carried out one time, and no attempt was made to optimize the application conditions or pretreatment of the adherend surface before spraying. Optimization of the application conditions could potentially improve the durability of plasma-sprayed coatings.

## 2. INTRODUCTION

The principal requirement for an adhesive bond is that the bond maintain its integrity in the structure under use conditions during the lifetime of the structure. Many components contribute to the strength and durability of an adhesive bond including the adhesive, the adherend, the surface preparation, the use conditions, and the bond geometry. For high performance applications the nature of the surface preparation often plays a dominant role for specimens exposed to severe environmental conditions. Many surface pretreatments involve the use of organic solvents and solutions containing carcinogenic transition metals. Manufacturing industries that rely on adhesive bonding, along with the EPA and other governmental and professional groups, seek surface pretreatments that are environmentally safe.

The role of the surface treatment of an adherend is to promote highly stable adhesive-adherend interactions; high stability is accomplished by making the chemistry of the adherend and adhesive compatible (1-5) so that robust oxides are present and weak boundary layers are removed. The common surface preparations used to enhance durability for adhesive bonding of metals include aqueous chromic-sulfuric acid treatment, aqueous ferric salt-sulfuric acid treatment, phosphoric and chromic acid anodization for aluminum, as well as, grit blasting and chromic acid or sodium hydroxide anodization for titanium (5). Although these methods for surface preparation result in strong durable bonds, they require the maintenance of chemical supplies, appropriate reaction vessels, and handling and disposing of waste. Furthermore, pretreatments such as phosphoric acid anodization (PAA) are unstable in hot wet conditions (6,7) and titanium alloys experience oxide dissociation at elevated temperatures (7-9). Also of concern is the reproducibility of surface chemistry and morphology of chemically prepared surfaces. Small changes in preparation conditions can result in large changes in bond strength and durability (10). Alternative surface preparations are needed to provide stability at high temperatures and to satisfy environmental regulations. Plasma spray techniques (11,12) may offer an appropriate



alternative method to prepare adherend surfaces for adhesive bonding. Plasma-spraying also offers the possibility of obtaining surfaces of different chemistry and morphology (5,11,12).

Plasma spraying has been used for decades to spray coatings for anti-corrosion, wear resistance, and thermal barriers (11-17). The fundamental process that occurs during plasma spraying is that a fine powder is introduced into a gas plasma at elevated temperatures where it becomes molten and is projected onto a substrate. After the molten particle impacts the substrate, it resolidifies, having properties much different than the original powder. Studies have shown that plasma-sprayed coatings adhere well to metal substrates due to interdiffusion of the coating components into the metal (18-21). This interdiffusion becomes even greater when a surface preparation such as grit blasting or gaseous plasma spraying (no powder injected) is used prior to spraying to roughen the surface and remove contaminants (7).

A potential advantage of plasma spraying for the treatment of adherends for adhesive bonding is that the chemistry of the coating can be changed to be compatible with the adhesive. This can be accomplished by spraying a powder that has the desired chemistry, or in low pressure systems, reactive gases can be introduced, which can react at high temperatures with the powder being sprayed (22).

Clearfield and coworkers (7) have described the use of plasma sprayed coatings for enhanced durability of bonded titanium. Titanium-6Al-4V alloy powder was plasma-sprayed on titanium-6Al-4V alloy adherends with the goal of obtaining a surface coating that would be stable at elevated temperatures. The plasma-sprayed coatings exhibited a micro-rough morphology and the surface morphology did not change upon exposure in a vacuum at 450°C (842°F) (7). Surface analysis of the plasma-sprayed coating indicated principally titanium dioxide. The studies demonstrated that bond durability, as determined via a wedge test, was equivalent to that for surfaces anodized in sodium hydroxide or chromic acid (7). The use of plasma-sprayed alumina ( $\text{Al}_2\text{O}_3$ ) coatings for adhesive bonding of composites,

aluminum and titanium has been reported by Pike, et al. (23). Alumina was plasma-sprayed to obtain a thin (50  $\mu\text{m}$ ; 0.002") and microporous coating. The durability of plasma-sprayed adherends compared favorably with that for aluminum and titanium adherends that had been pretreated, respectively, via phosphoric acid anodization and Pasa-Jell 107 procedures. Davis and associates (24) recently compared the durability of solution-treated aluminum and titanium with specimens that had been plasma-sprayed with a variety of inorganic compounds, inorganic/polymer mixtures, and polymers. A general finding was that a coating prepared by plasma-spraying an aluminum-silicon alloy mixed with a polyester onto aluminum exhibited good dry and hot-wet durability (24). Davis and coworkers (24) reported on dry and hot-wet durability of aluminum that had been plasma-sprayed with a polyester, PEEK, and mixtures of aluminum and polymers and bonded with epoxy adhesives. Some of the coated/bonded aluminum exhibited performance and failure modes under dry conditions equivalent to that for solution-prepared surfaces. On the other hand, under hot-wet conditions the polymer-coated specimens failed in the coating, at the coating-substrate interface, or at the coating-adhesive interface.

The purpose of the current investigation (25,26) was to plasma-spray aluminum and titanium adherends using a variety of materials to obtain a different surface chemistry and to characterize the surfaces in preparation for investigation of the durability of adhesively bonded metal adherends. A principal goal was to obtain plasma-sprayed inorganic and polymeric materials that might be effective as surface treatments for high performance adhesive bonding. Although inorganic materials have been plasma-sprayed in adhesive bonding studies (7,23,24) no detailed investigation of plasma-sprayed polymeric materials as a surface preparation for adhesive bonding has appeared in the literature. The focus of this investigation is on characterization of the plasma-sprayed adherends to determine the morphology and chemical stoichiometry of the plasma-sprayed coatings. The coating materials include inorganic oxides that are acidic and basic and polymeric materials that contain a variety of functional groups. These materials were selected to permit an inquiry into the

influence of acid-base characteristics on the durability of adhesively bonded metals. An additional purpose of the current study was to plasma-spray aluminum and titanium adherends using a variety of polymeric materials to obtain a variety of surface chemistries (26). A principal goal was to obtain plasma-sprayed polymeric materials that might be effective as surface treatments for high performance adhesive bonding. The polymeric coating could provide modulus or stress relief between the adherend and the polymer adhesive. Ultimately, plasma-sprayed coatings could provide a method of applying adhesive to adherends for subsequent adhesive bonding. Thus inorganic compounds, polymeric materials, and mixtures of polymeric materials have been plasma-sprayed on aluminum and titanium. Plasma-spray-coated aluminum and titanium using inorganic and organic materials were bonded with an epoxy or a polyimide adhesive.

### 3. EXPERIMENTAL SECTION

#### 3.1 Materials

Aluminum 6061 and titanium-6Al-4V alloys were used as adherends. Aluminum 6061 plates were purchased from McMaster-Carr Supply Co., New Brunswick, NJ. Titanium-6Al-4V specimens were obtained from President Titanium, Hanover, MA. The specimen dimensions for aluminum were 2.5 cm X 10.2 cm X 0.64 cm (1" X 4" X 0.25") and for Ti were 2.5 cm X 10.2 cm X 0.23 cm (1" X 4" X 0.090"). The plasma-sprayed area on each specimen was 2.5 cm X 7.6 cm. (1" X 3").

Hex-head Al 2024-T4 and hex-head titanium-6Al-4V bolts, used for the butt torsion specimens, were purchased from commercial suppliers. The bolts were 5 cm (2") in length and 0.95 cm (0.375") in diameter.

Plasma spraying of adherends with inorganic coatings was carried out at Engineered Coatings, Rocky Hill, CT. The selection of coatings was based on the desire to obtain different acid/base surface chemistries on the adherends. Specimens were grit blasted with silicon carbide before applying the plasma-sprayed coatings.  $\text{Al}_2\text{O}_3$ ,  $\text{AlPO}_4$ ,  $\text{MgO}$ , and  $\text{SiO}_2$  were plasma-sprayed on aluminum adherends, and  $\text{TiO}_2$ ,  $\text{TiSi}_2$ ,  $\text{MgO}$ , and  $\text{SiO}_2$  were deposited on titanium adherends. All inorganic coatings, except  $\text{SiO}_2$ , were sprayed to obtain 25  $\mu\text{m}$  (0.001") and 150  $\mu\text{m}$  (0.006") coating thicknesses.  $\text{SiO}_2$  could not be deposited at 150  $\mu\text{m}$  (0.006") due to failure of the material to adhere to itself.  $\text{SiO}_2$  coating thicknesses were 25  $\mu\text{m}$  (0.001") and 50  $\mu\text{m}$  (0.002"). In the preparation of the  $\text{AlPO}_4$  coating it was necessary to add silica as a flow agent to the powder upon introduction into the plasma. Thus, the analytical data presented for  $\text{AlPO}_4$  do not correspond to pure aluminum phosphate. **Table 1** lists the powders, selected properties of the materials, and the suppliers.

Table 1. Inorganic Powders and Suppliers

<u>Powder</u>	<u>Mesh size</u>	<u>M.P.°C</u>	<u>Purity(%)</u>	<u>Supplier</u>
Al <sub>2</sub> O <sub>3</sub>	-25 +5	2000	98	Metco 105SF
AlPO <sub>4</sub>	-44 +5	>1500	unknown	City Chemical
SiO <sub>2</sub>	-44 +10	1700	99.9	Atlantic Equipment
MgO	-44 +10	2850	95	Cerac; M1139
TiO <sub>2</sub>	-53 +10	1830	99	Metco 102
TiSi <sub>2</sub>	-105 + 44	1760	99.9	Atlantic Equipment

Plasma spraying of polymers was carried out at Applied Polymer Systems (APS), Tampa, FL. Before plasma spraying, the metal adherends were grit-blasted with alumina (#80 grit) at 60 psi, and were then wiped with methyl ethyl ketone (MEK). Pure argon was used in the plasma torch. Powders were introduced into the plasma torch using a fluidized bed or a rotary hopper. The spraying was carried out to obtain a coating thickness in the range of 75  $\mu$ m to 125  $\mu$ m (0.003" to 0.005"). **Table 2** lists the polymers that were sprayed and the suppliers of the polymers.

Table 2. Polymer Powders and Suppliers

<u>Polymer</u>	<u>Supplier</u>
Epoxy: Everclear	Fuller O'Brien
Polyester: crystal clear	Fuller O'Brien
Cyanate ester: PT 60 (CE)	Allied Signal
LaRC-TPI 1500, polyimide	Mitsui-Toatsu
Bismaleimide (BMI)	Shell Chemical

The epoxy and polyester powders were sprayed onto aluminum and titanium without problems. Pure LaRC-TPI polyimide flowed easily through the plasma gun, but decomposed under a number of experimental conditions. To alleviate the decomposition problem and obtain a polyimide-containing coating, a 1:1 (w:w) physical mixture of BMI and LaRC-TPI was sprayed onto aluminum and titanium. Similarly, to obtain a coating of the cyanate ester it was necessary to spray a 2:3 (w:w) mixture of BMI and CE.

Aluminum and titanium adherend surfaces were also pretreated using conventional solution surface preparations. Aluminum was anodized in 15% (w/w) phosphoric acid for 20 minutes at a current density of 129 amps/m<sup>2</sup> (12 amps/ft<sup>2</sup>). Titanium was treated in Turco 5578 solution (37.6 g/1000 mL) H<sub>2</sub>O at 70-80°C (158-176°F) for 5 min. and then rinsed in DI water for 5 min. Following the initial cleaning treatment specimens were etched in a more concentrated Turco 5578 solution, 360 gm./1000 mL H<sub>2</sub>O, at 80 - 100°C (176-212°F) for 10 min. Titanium was then rinsed in DI water at 60 - 70°C (140-158°F). All treated samples were stored in a desiccator until bonded. The Turco treatment for titanium butt-torsion samples followed the same procedure as for the titanium wedge-type specimens.

Plasma-sprayed and solution-treated adherends were bonded in a wedge configuration (27) and a butt-torsion configuration using a 3M AF-191 epoxy film adhesive or an American Cyanamid (Cytec) polyimide adhesive (FM-36). The bond-line thickness for all samples was 0.25 mm (0.010"). Specimens were bonded according to procedures outlined by the manufacturers as summarized below.

AF-191: Primer solution (Scotchweld EC-3917) was applied to solution-treated adherends using a paint brush. The coating was allowed to cure at room temperature for 30 min. The specimen was then heated in a forced air oven at 120°C (248°F) for 30 min. The primer solution was only applied to PAA and Turco 5578 specimens when bonding with the epoxy adhesive. No primer was used in bonding the plasma-sprayed adherends. Epoxy adhesive film (AF-191) was positioned between the adherends and the specimen was placed on the press platen which had been heated to 93°C (200°F).

A pressure of 40 psi was applied and the specimen was heated at a rate of 17°C/min (30°F/min.) to 177°C (350°F). After reaching 177°C (350°F), the samples were held at this temperature for 60 min. The specimens were then cooled at a rate of 6°C/min (10°F/min) to 93°C (200°F) before removing the pressure. Bonded samples were removed from the press and placed in a desiccator until initiating the environmental durability tests.

FM-36: Polyimide adhesive film was positioned between the adherends and the specimen was placed on the press platen that had been heated to 93°C (200°F). A pressure of 40 psi was applied and the specimen was heated to 177°C (350°F) and was held at this temperature for 60 min. The samples were then cooled to 93°C (200°F) before removing the pressure. The specimens were then post-cured by placing them in an oven at 260°C (500°F) for 3 hrs. Bonded samples were removed from the press and placed in a desiccator until starting the environmental durability tests.

### 3.2 Chemical Surface Treatments: Butt-torsion specimens

Prior to surface treatment of the butt-torsion samples, all of the bolt ends were machined to the same length to smooth and flatten the surfaces. This was done to obtain a uniform bondline thickness and to remove surface lips that would reduce the strength of the bond. Hex-head bolts for the butt torsion studies were plasma-sprayed in a manner identical to that for the preparation of wedge-type adherends. Butt-torsion specimens were bonded using a rack especially designed to maintain alignment of the bolts and to allow the application of bonding pressure. The rack is shown in **Figure 1**.

Cleaning - Prior to further surface treatment, all of the aluminum bolts were cleaned by submersion in 5% (w/w) aqueous NaOH at 60°C for three minutes followed by a one minute rinse in 50% (v/v) aqueous solution of HNO<sub>3</sub> and a two minute rinse in DI water.

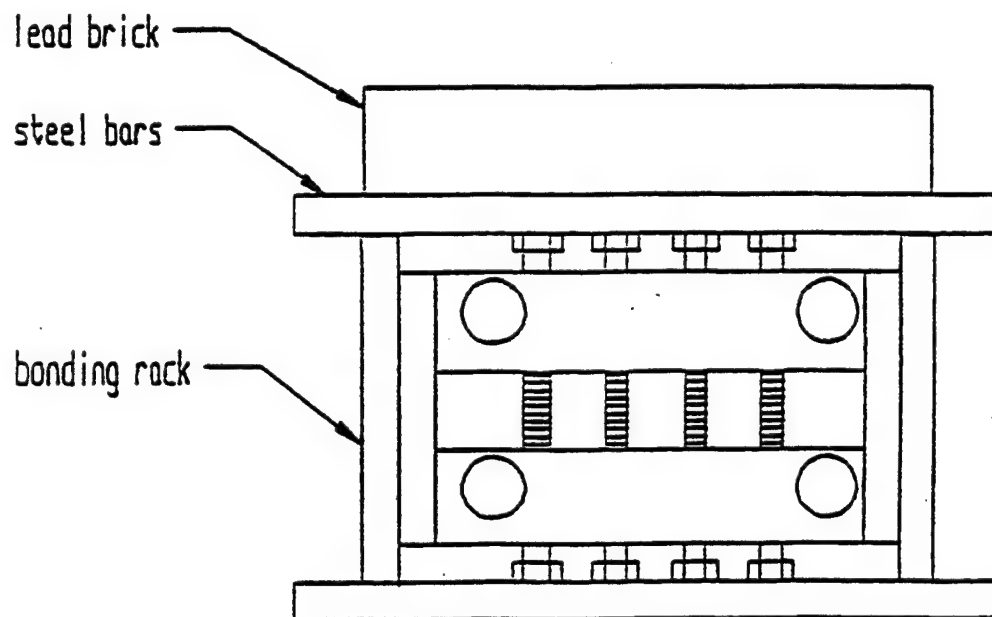
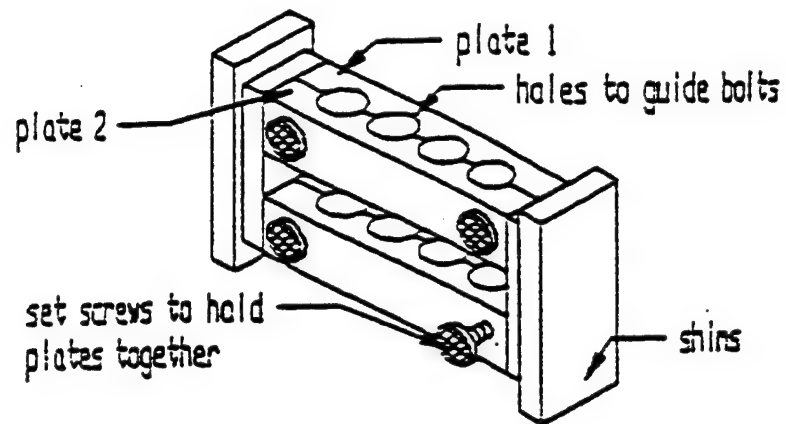


Figure 1. Bonding rack for the preparation of butt-torsion specimens.



Phosphoric Acid Anodization - The cleaned aluminum bolts were anodized in a 15% (w/w) aqueous solution of  $\text{H}_3\text{PO}_4$  at 129 amps/m<sup>2</sup> (12 amps/ft<sup>2</sup>) for 20 minutes. During the anodization process, the temperature of the phosphoric acid solution was maintained between 25°C (77°F) and 28°C (82°F) using an ice bath. The bolts were rinsed in DI water for two minutes following anodization. The bolts were then placed in a desiccator until primed or bonded.

Vinyl Phosphonic Acid Treatment - Cleaned aluminum bolts were initially submerged in a boiling aqueous ammonium hydroxide solution, with a pH of about 9.5, for 1 minute. This was followed by dipping the bolts in a 0.01 molar vinyl phosphonic acid solution at 50°C (122°F) for 10 seconds. The bolts were then rinsed in deionized water for 2 minutes and placed in a desiccator until primed or bonded.

P2 Etch - Cleaned bolts were placed in a P2 solution at 63°C (145°F) for 8 minutes. The P2 solution consisted of 122.5 g  $\text{Fe}_2(\text{SO}_4)_3 \cdot 4\text{H}_2\text{O}$  in 0.185 L of con.  $\text{H}_2\text{SO}_4$  diluted to 1 L with  $\text{H}_2\text{O}$ . The bolts were then rinsed in deionized water for 2 minutes and stored in a desiccator until primed or bonded.

In the durability evaluation, wedge and butt torsion specimens were exposed to an environmental cycle (26). The cycle was designed to represent potential use conditions for these adhesively-bonded materials. Samples were exposed to cycle A for 100 hrs, and then to cycle B conditions for the duration of the durability experiments (approximately 3500 hrs).

Environment	Cycle A	Cycle B
cold; - 20°C (-5°F)	2 hrs.	24 hrs
air, 70% RH; 66°C (151°F)	2 hrs.	24 hrs.
dry air; 160°C (320°F)	2 hrs.	24 hrs.
vacuum, 130 torr; 160°C (320°F)	2 hrs.	24 hrs.
room tempt.; 23°C (73°F)	16 hrs.	24 hrs.

Crack growth was measured after each step in the exposure cycle. The crack growth measurements were accurate to within  $\pm 2$  mm. ( $\pm 0.08$ "), and the reproducibility of the initial crack lengths among specimens with the same coating was  $\pm 10$  mm ( $\pm 0.4$ ") for aluminum and  $\pm 5$  mm ( $\pm 0.2$ ") for titanium. The results presented in the figures represent average growth data for five specimens of each treatment and adherend. Butt torsion specimens were placed in the durability test apparatus shown in **Figure 2** during exposure to the environmental cycle. Chemically cleaned aluminum specimens were torqued at various levels in the experiments. The bonded samples in the plasma spray study were loaded to 20 percent of the failure load of standard specimens and exposed to a cycle of cold, hot humid, hot dry, hot vacuum, and ambient laboratory environments. Twenty percent load was exerted because joints are typically design to carry 20 to 40 percent of their failure load and the cyclic environment was meant to simulate the service conditions of an airplane.

Plasma-sprayed adherends and failure surfaces were characterized using XPS and SEM. XPS spectra were measured using a PHI Perkin-Elmer Model 5400 photoelectron spectrometer. Photoelectrons, generated using Mg  $K_{\alpha}$  radiation ( $h\nu = 1253.6$  eV), were analyzed in a hemispherical analyzer, and detected using a position sensitive detector (25,28-30). The binding energy scale was calibrated in reference to the carbon 1s peak for background carbon. In the presentation of the elemental results, photoelectron spectral peak areas were measured and subsequently scaled to account for ionization probability and an instrumental sensitivity factor to yield results which are indicative of surface concentration in atomic percent (25,29). The elemental compositional data were obtained by taking the average of at least three individual measurements. The precision and accuracy for the concentration evaluations are, respectively, about 10% and 15%. Multi-component carbon 1s photopeaks were curve fitted using photopeaks of Gaussian peak shape with a full-width-at-half maximum (FWHM) of  $1.6 \pm 0.1$  eV. The C 1s binding energy values were selected to correspond to carbon-carbon, carbon-hydrogen, and carbon-oxygen-containing functional groups (25,28,29).

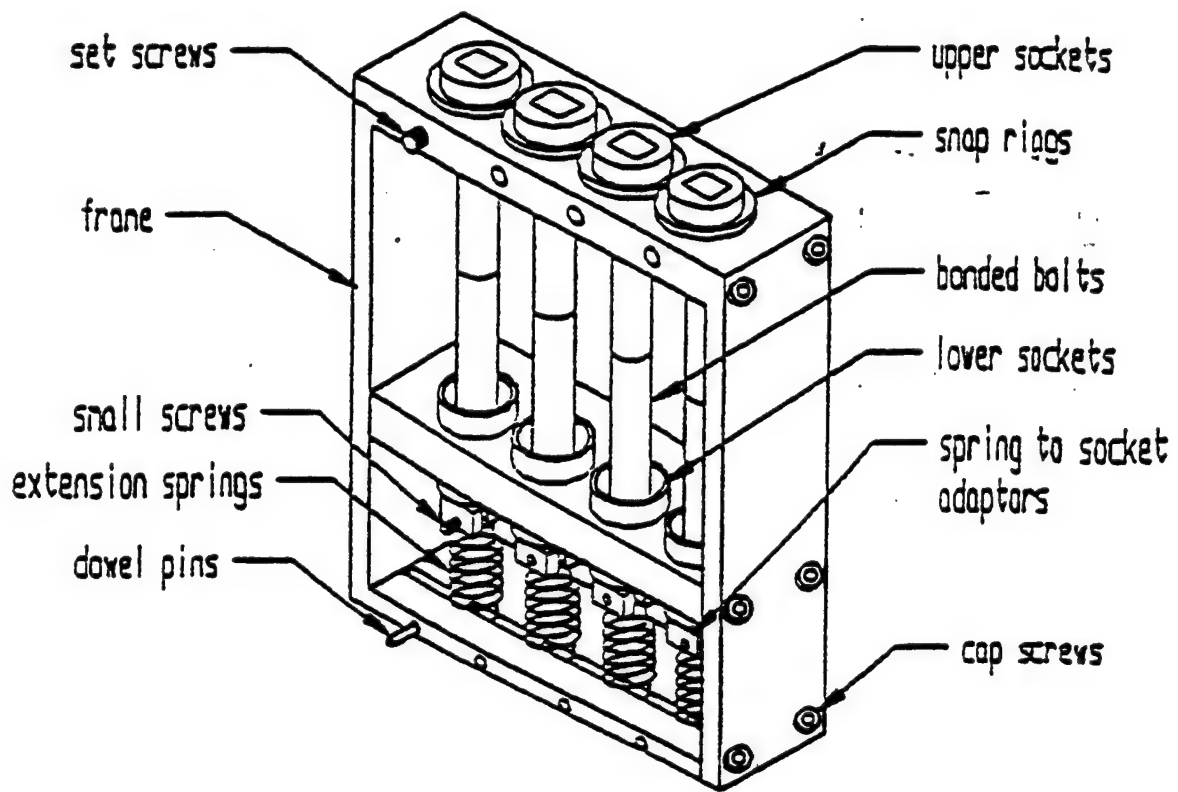


**Figure 2. Durability testing apparatus for butt-torsion specimens.**

SEM photomicrographs were determined using an ISI Model SX-40 scanning electron microscope. Samples were sputter-coated with a thin gold film ( $\sim 200 \text{ \AA}$ ; 20 nm).

## 4. Plasma-Sprayed Adherends - Surface Characterization of Aluminum and Titanium

### 4.1 SEM Characterization

Scanning Electron Microscopy (SEM) was used to investigate the topographical features of the plasma-sprayed coatings. The SEM photomicrographs revealed significant morphological differences when comparing the organic and inorganic plasma-sprayed coatings and also when comparing the features among the inorganic coatings. An SEM photomicrograph for the polyester-sprayed coating on titanium is shown in **Figure 3**. The coating is smooth with few distinguishing features. The features exhibited in **Figure 3** were characteristic of the polyester, epoxy, and CE/BMI plasma-sprayed coatings. Among these three sprayed coatings the topographical features were indistinguishable. The surface features for the TPI/BMI plasma-sprayed coating, as revealed from the SEM photomicrograph in **Figure 4**, were unique compared to those for the other three polymeric coatings. The TPI/BMI coating was rough and cavernous and exhibited nodular particle-like features that were 25 to 30  $\mu\text{m}$  (0.001-0.0012") in diameter. The surface appears to have particles stacked on top of one another. Thus the preparation of the plasma-sprayed polymeric coatings yields smooth and rough-cavernous features. The findings suggest that the mode of coating formation may be different for the TPI/BMI specimen. No attempt was made to discover the operational parameters or application conditions that led to the differences in the features of the polymeric coatings. No significant differences were noted in coating morphology when comparing the same coatings on aluminum or titanium.

The SEM photomicrographs for the plasma-sprayed inorganic coatings are shown in **Figures 5-10**. Some of the inorganic coatings exhibited the splattering effect which is a common characteristic of plasma-sprayed coatings (11,12,31) The splattering characteristics were particularly evident for the  $\text{Al}_2\text{O}_3/\text{Al}$ ,  $\text{AlPO}_4/\text{Al}$ , and  $\text{TiO}_2/\text{Ti}$  coatings **Figures 5-7**. The SEM photomicrographs for the other plasma-sprayed inorganic coatings (**Figures 8-10**)  $\text{MgO}/\text{Al,Ti}$ ;  $\text{SiO}_2/\text{Al,Ti}$ ; and  $\text{TiSi}_2/\text{Ti}$

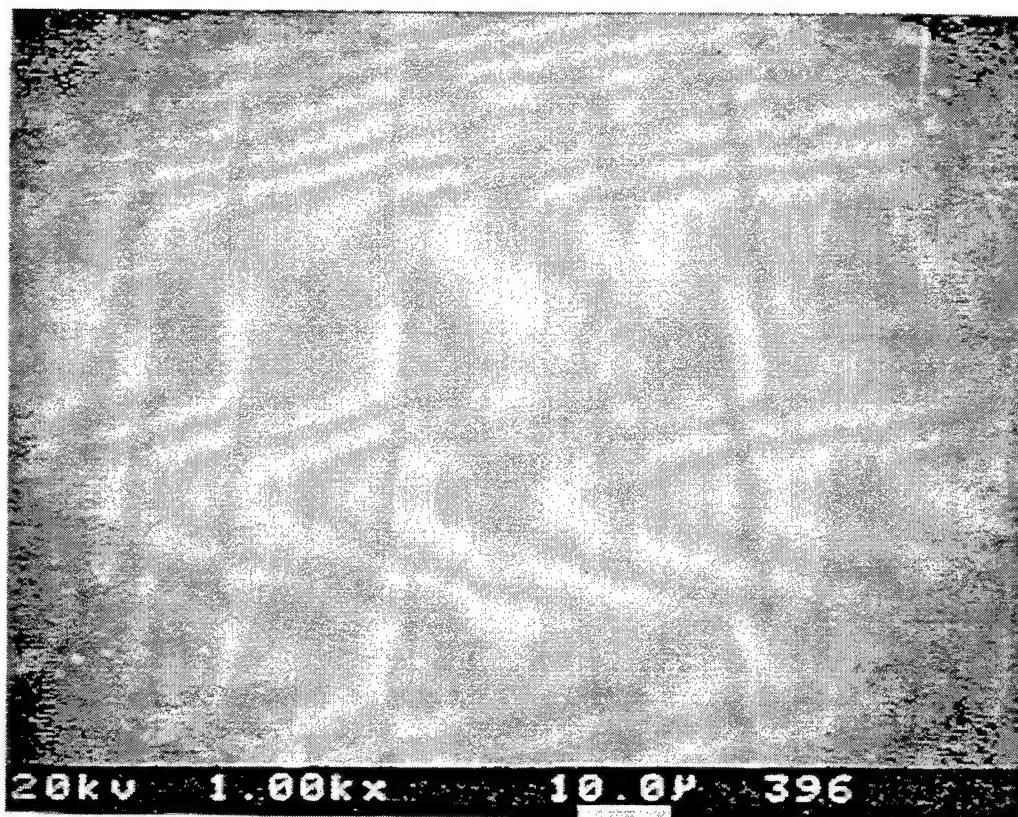


**Figure 3.** Scanning electron photomicrograph of polyester powder plasma-sprayed on titanium.

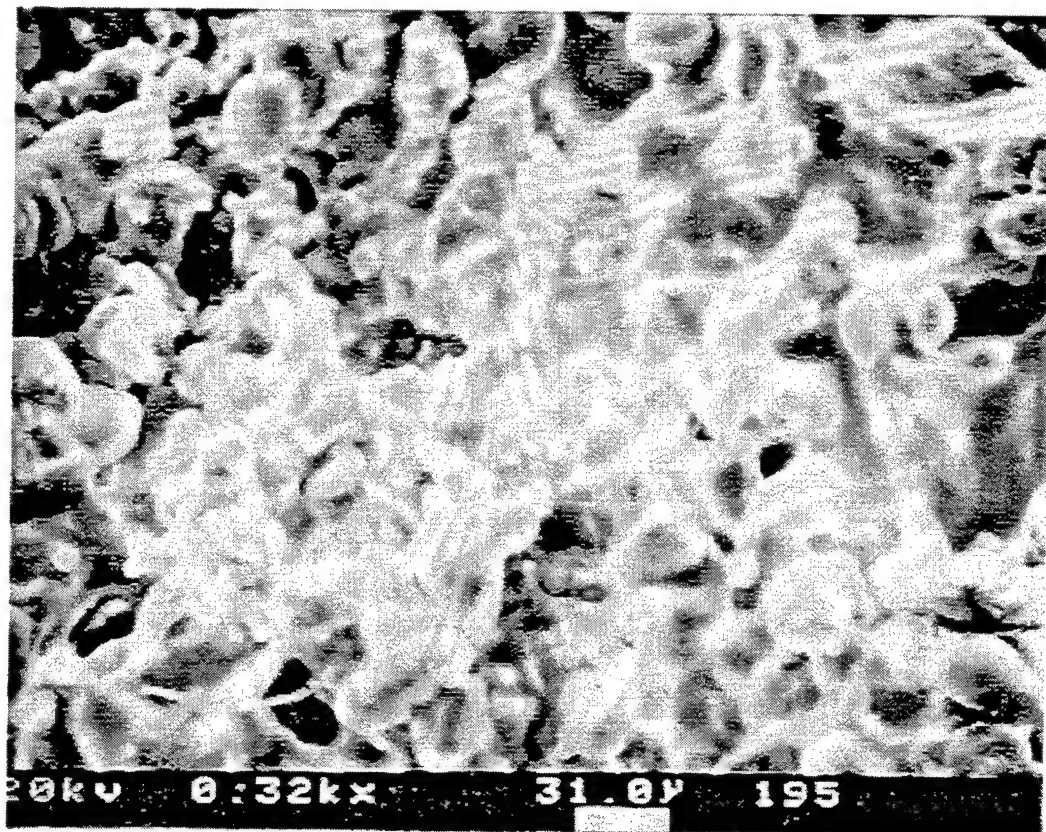


**Figure 4.** Scanning electron photomicrograph of Bismaleimide-LaRC-TPI powder mixture plasma-sprayed on titanium.



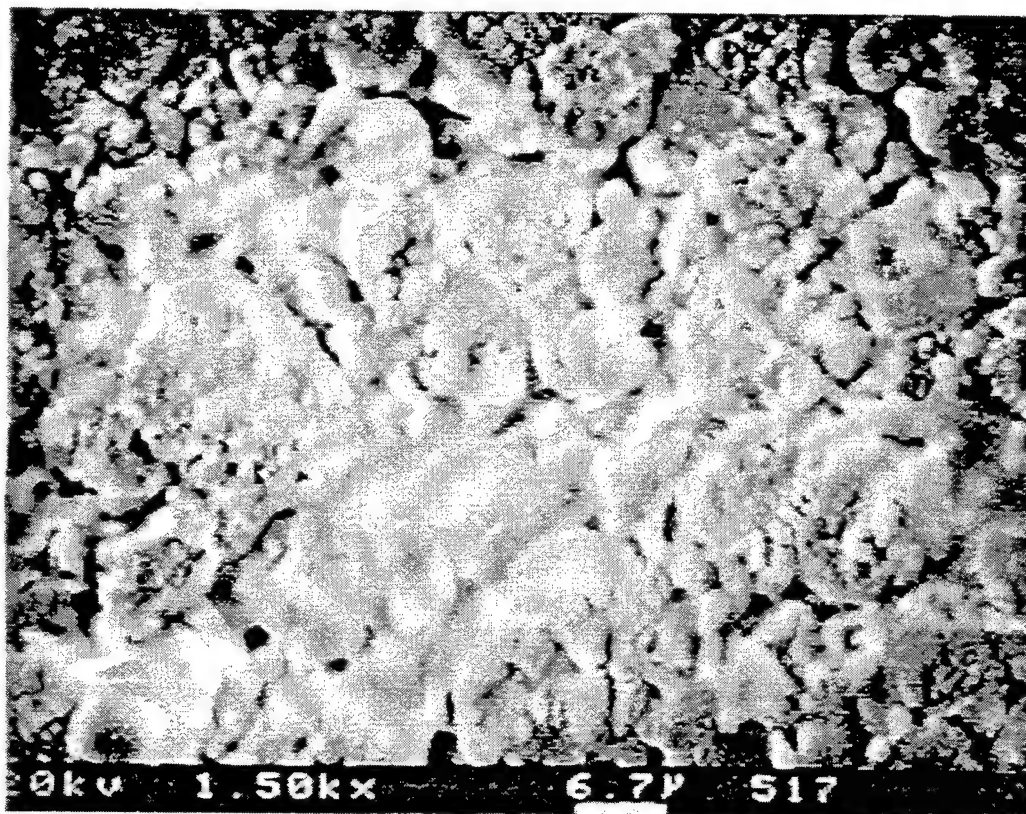


**Figure 5.** Scanning electron photomicrograph of Al<sub>2</sub>O<sub>3</sub> powder plasma-sprayed on aluminum



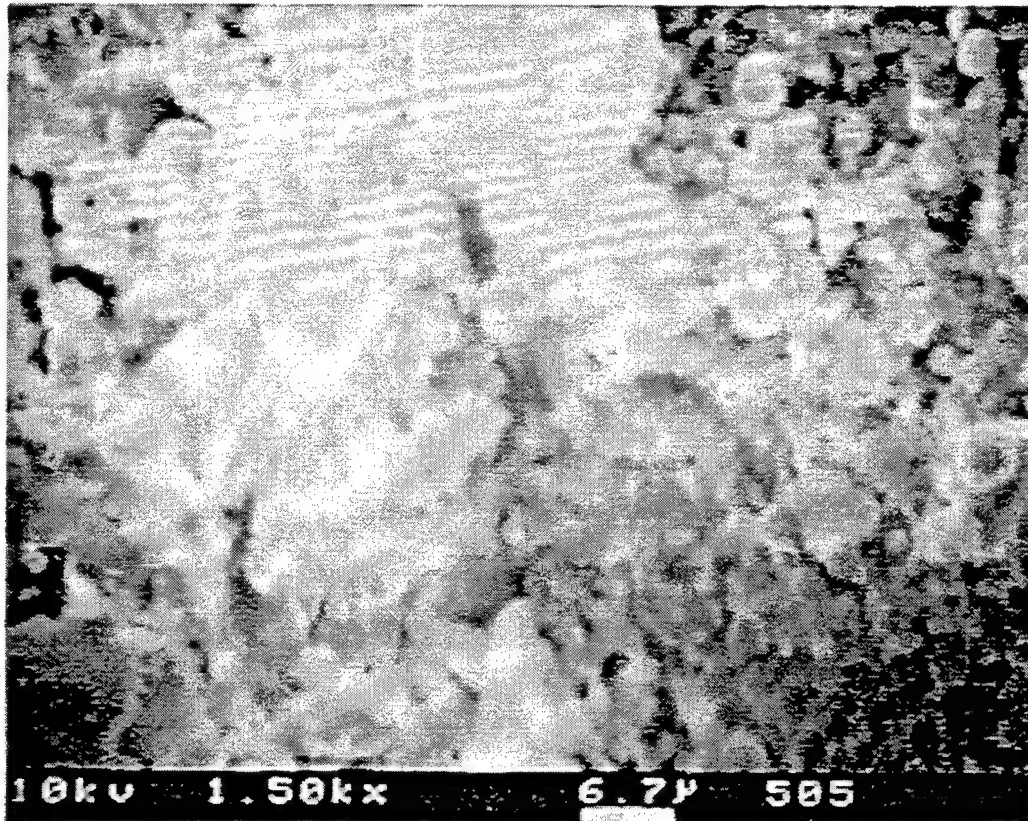


**Figure 6.** Scanning electron photomicrograph of AlPO<sub>4</sub> powder plasma-sprayed on aluminum.

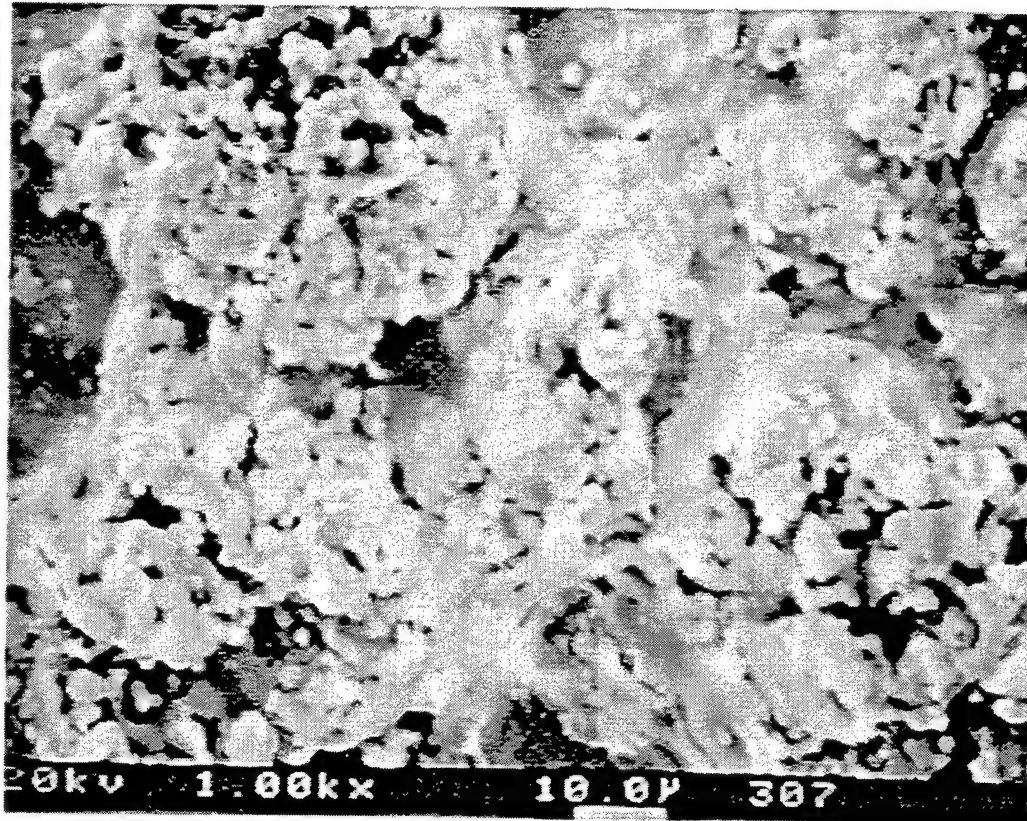


**Figure 7.** Scanning electron photomicrograph of  $\text{TiO}_2$  powder plasma-sprayed on titanium.

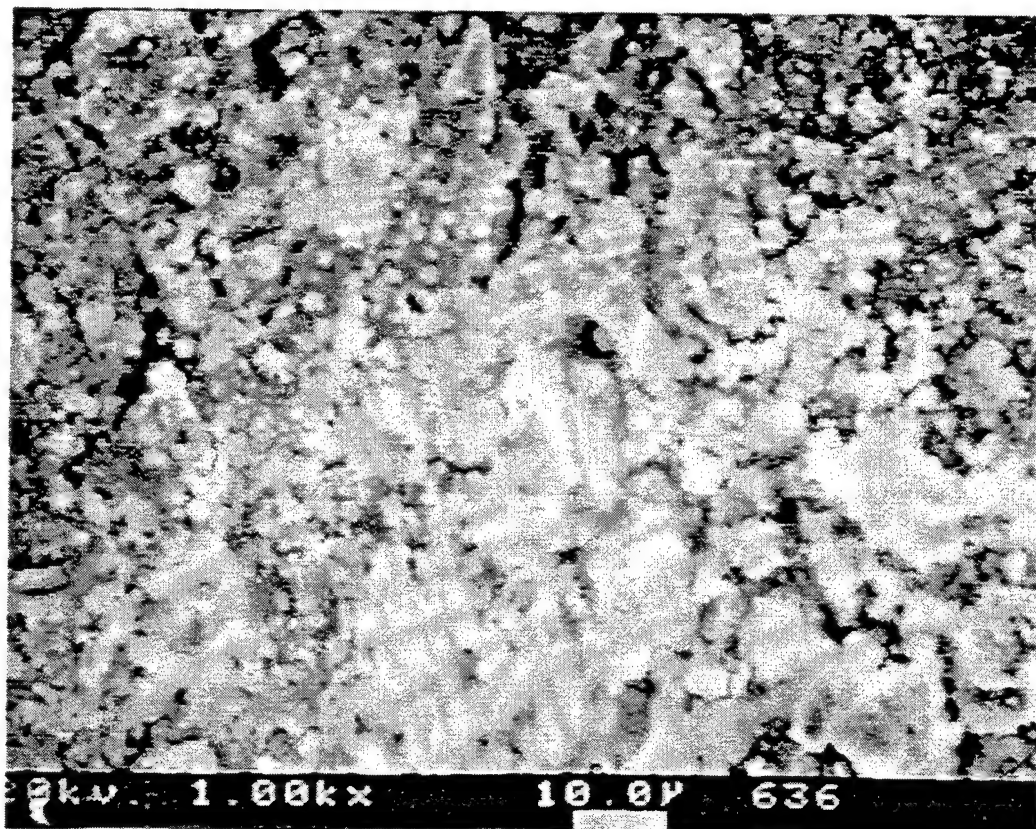
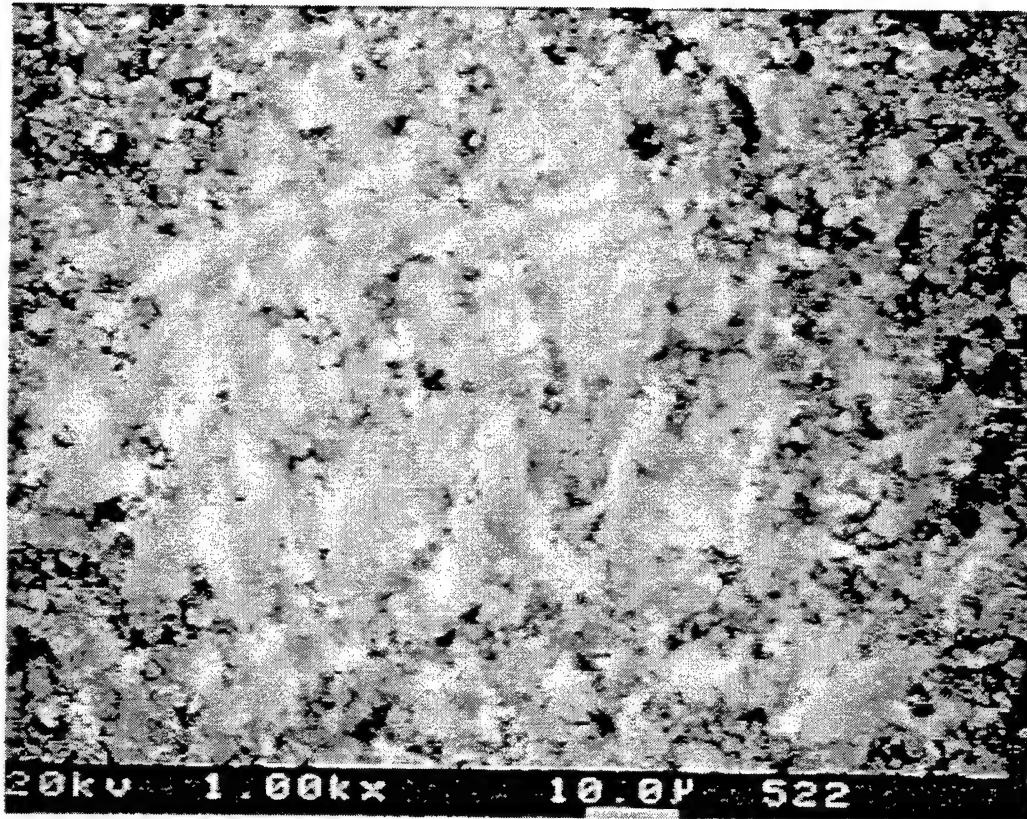
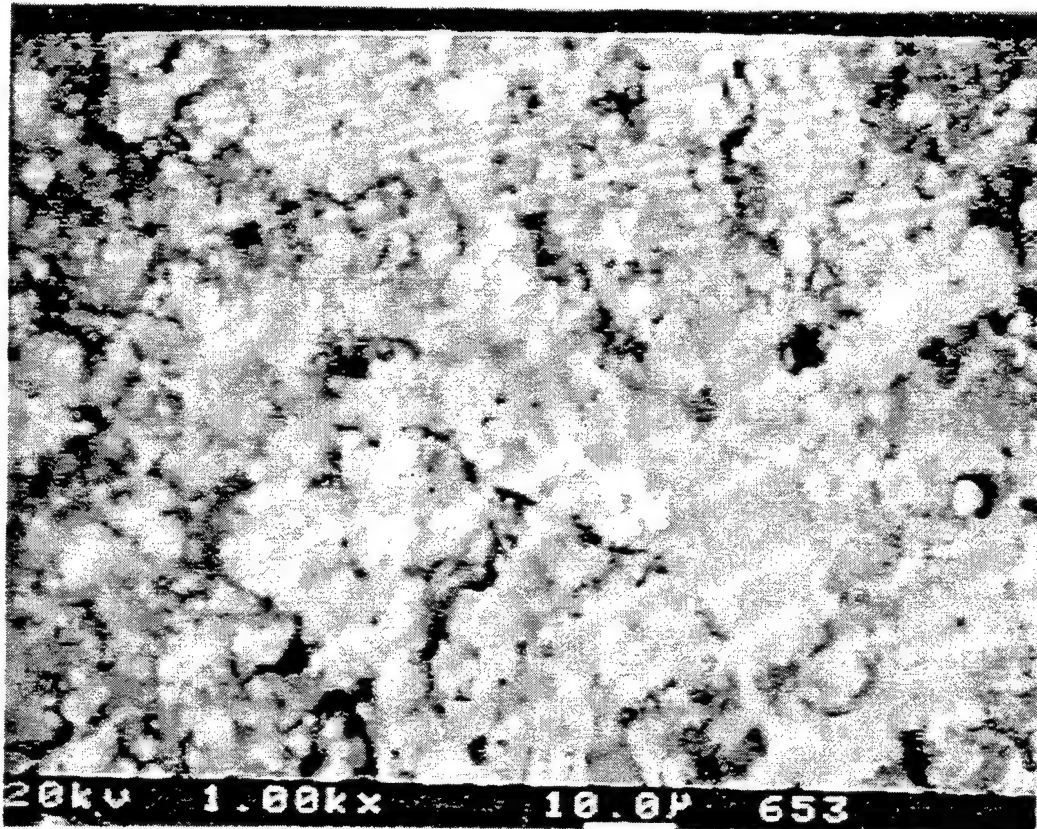


Figure 8. Scanning electron photomicrograph of MgO powder plasma-sprayed on aluminum.



**Figure 9.** Scanning electron photomicrograph of SiO<sub>2</sub> powder plasma-sprayed on aluminum.



**Figure 10.** Scanning electron photomicrograph of TiSi<sub>2</sub> powder plasma-sprayed on titanium.



exhibited both smooth and rough features. No significant differences in coating morphology were noted when comparing the same coating, MgO or SiO<sub>2</sub>, on aluminum or titanium. Also there were no differences in topography when comparing specimens coated with the same material at different thicknesses.

#### 4.2 XPS Characterization

The powders and plasma-sprayed specimens were analyzed by XPS to obtain information regarding chemical surface composition, to inquire about possible chemical changes resulting from the spraying process, and to obtain base-line data for use in establishing failure modes in subsequent durability experiments. **Table 3** summarizes the XPS atomic percent composition results for the organic-polymeric powders and for the corresponding sprayed coatings. A comparison of the XPS data for the polymer powder and for the plasma-sprayed polymers (**Table 3**) suggests that some change has taken place during plasma spraying. The change is evident by the general decrease in carbon content and the increase in the concentration of oxygen and nitrogen on the sprayed specimens compared to the results for the powders. The presence of silicon in some of the plasma-sprayed specimens is a result of the incorporation of small amounts of silica (SiO<sub>2</sub>) contamination in the spraying chamber. The presence of silica also contributes to the increased oxygen content in the plasma-sprayed specimens. Fluorine as an organic fluoride was detected in the epoxy powder, but was removed in the spraying process and does not appear on the surface of the plasma-sprayed epoxy. The increase in nitrogen content among the sprayed epoxy and polyester samples is likely due to some reaction of the materials with nitrogen in the air outside of the plasma spraying region.

To explore possible changes in chemical functionality for epoxy and polyester plasma-sprayed specimens, carbon 1s spectra were curve fitted. Representative curve fitted C 1s spectra are presented for epoxy and polyester in **Figures 11 and 12**, respectively. In the figures spectra are compared for the polymer powder and the

plasma-sprayed specimen. In the fitted spectra for the plasma-sprayed epoxy material evidence is obtained for C-H/C-C, C-O, and C=O functional groups, whereas in the

**Table 3.** XPS Characterization Results for Organic-Polymer Plasma-Sprayed Materials (atomic percent)\* [P = powder; PS = plasma-sprayed coating]

Polymer	C 1s		O 1s		N 1s		Si 2p		F 1s	
	P	PS	P	PS	P	PS	P	PS	P	PS
Epoxy	78.7	70.2	16.3	20.7	1.5	4.9	nd	4.2	3.5	nd
Polyester	77.3	65.1	22.1	25.3	0.6	5.3	nd	1.3	nd	nd
CE/BMI	81.1	77.0	11.5	13.9	7.4	6.1	nd	3.0	nd	nd
TPI/BMI	77.6	70.9	18.6	22.4	3.8	6.7	nd	nd	nd	nd

nd=element not detected; atomic % < 0.2%.

\*The results, labeled P, for CE/BMI and TPI/BMI are for pure powder before spraying, whereas the data, labeled PS, for CE/BMI and TPI/BMI are for the plasma-sprayed specimens which were obtained by spraying a physical mixture of the polymers.

powder only C-H/C-C and C-O functional groups are evident. The percent composition for the oxygen-containing functional groups is only slightly greater for the plasma-sprayed specimens. The appearance of the carbonyl functionality arises via oxidation either in the plasma or after deposition via reaction with air. A general result is that some oxidation of the epoxy material has occurred.

The C 1s spectra for polyester powder could be fitted by including C-H/C-C, C-O, and -O-C=O functional groups whereas the spectra for the plasma-sprayed specimen could be fit using C-H/C-C, C-O, C=O, and -O-C=O functional groups. To obtain reasonable fits for the C 1s spectra for the plasma-sprayed polyester, it was necessary to increase the concentration of the C-O group and to include a contribution

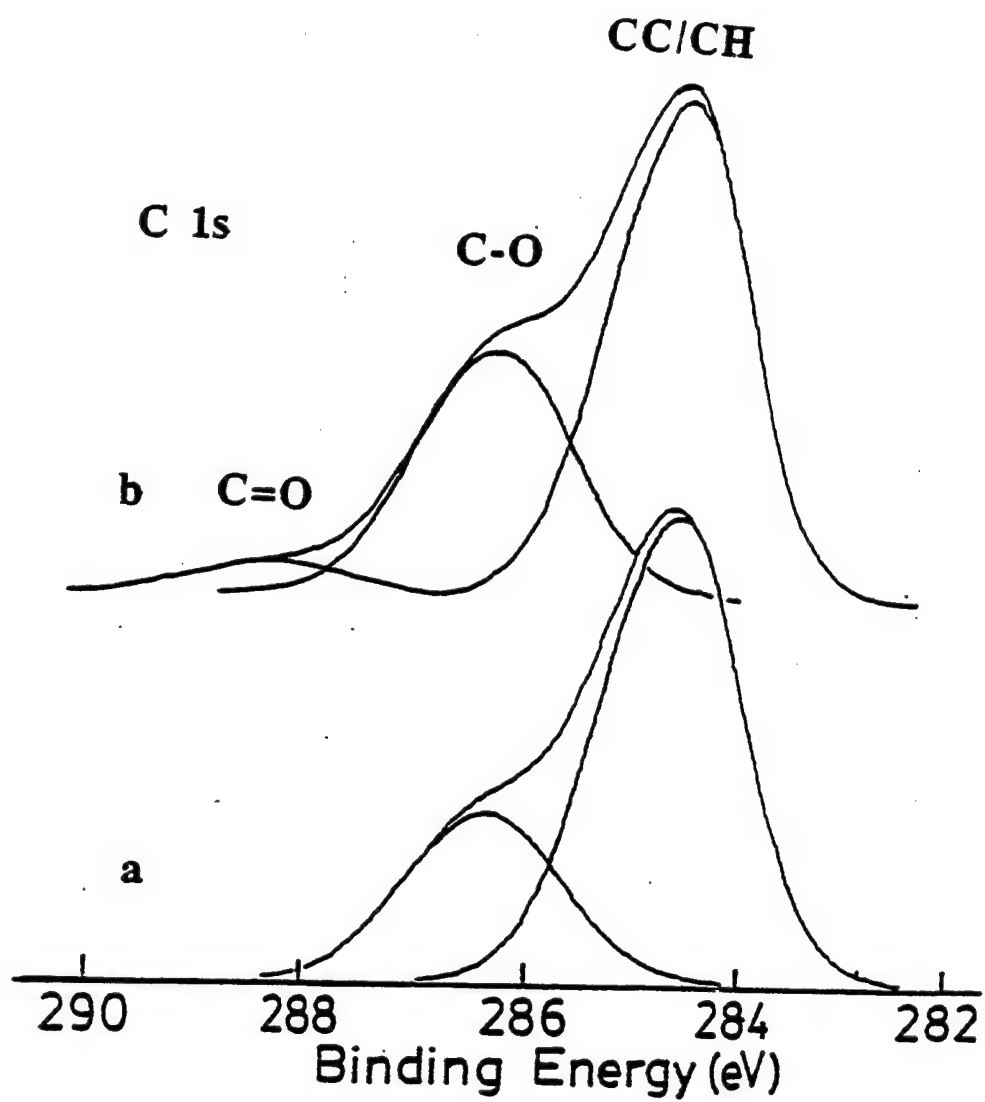


**Figure 11.** Carbon 1s x-ray photoelectron spectra for: a) epoxy polymer powder; b) epoxy polymer powder plasma-sprayed on titanium.



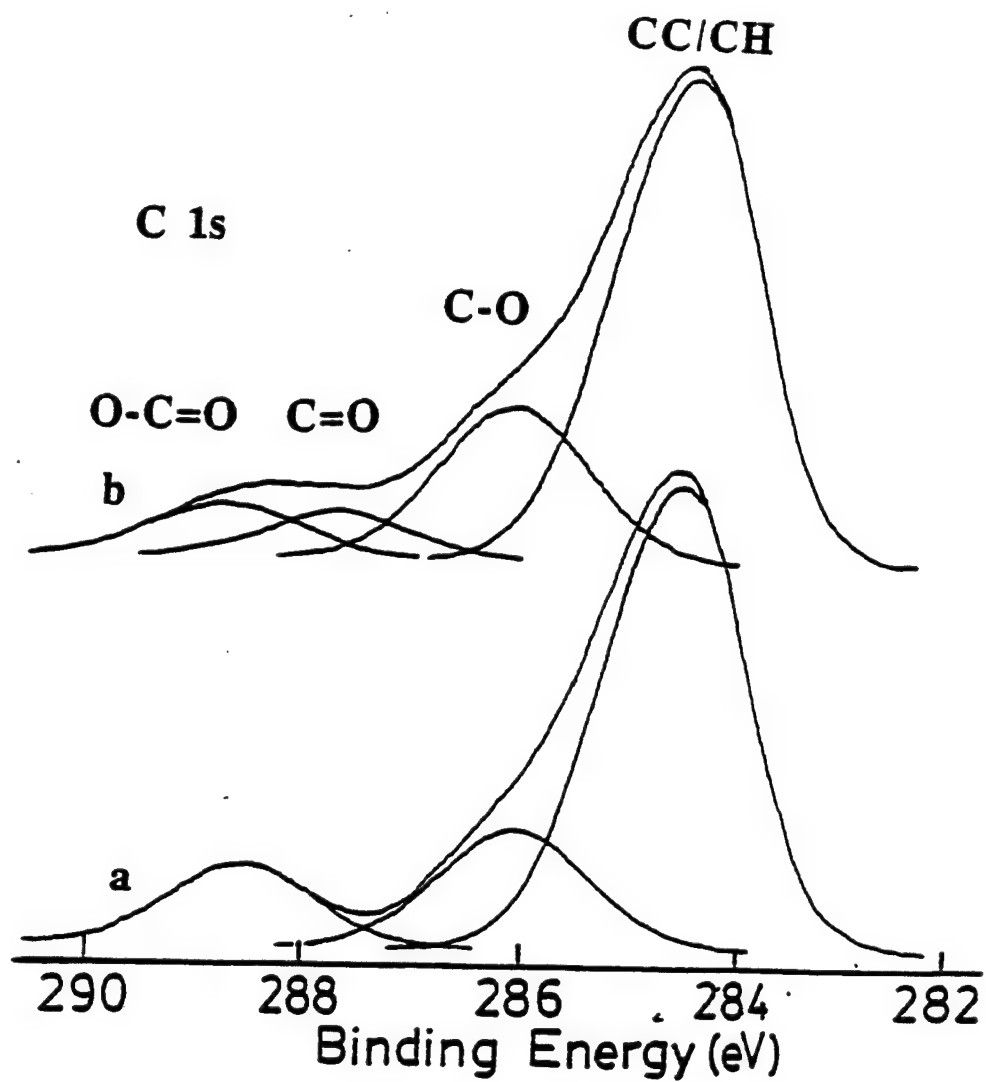


**Figure 12.** Carbon 1s x-ray photoelectron spectra for: a) polyester polymer powder; b) polyester polymer powder plasma-sprayed on titanium.

from a carbon doubly bound to oxygen (carbonyl) functional group as shown in **Figure 12**. The functional group distribution in the polyester indicates that the carboxyl group content has decreased leading to carbonyl-type group contribution. Alternatively, oxidation of the hydrocarbon or ether portion of the polyester could have taken place. Nevertheless, the compositional changes are small and the comparisons of functional group distributions of oxygen-containing groups for the powder and the plasma-sprayed samples indicate that little degradation of the plasma-sprayed materials has occurred. A detailed XPS functional group analysis, via curve fitting, for the cyanate ester- and LaRC-TPI-BMI mixtures was not carried out due to the complexity of the composition in the plasma-sprayed coating. Studies are in progress via other means to determine the component distribution in the sprayed coating.

The XPS surface characterization results for inorganic plasma-sprayed coatings are presented in **Tables 4 and 5**. The table for plasma-sprayed specimens shows only one entry for MgO and SiO<sub>2</sub> although these oxides were sprayed on aluminum and on titanium. The results for MgO and SiO<sub>2</sub> sprayed on the two different substrates were equivalent, so only data for coatings on aluminum are presented.

**Table 4.** XPS Results for Inorganic Powders  
(atomic percent)

Compound	C 1s	O 1s	Na 1s	Ti 2p	Al 2p	Si 2p	P 2p*/Mg 2p#
Al <sub>2</sub> O <sub>3</sub>	23.7	44.7	4.8	nd	21.5	5.3	nd
AlPO <sub>4</sub>	25.3	47.7	3.2	nd	11.9	nd	11.9*
MgO	22.0	49.8	0.5	nd	nd	3.9	23.8#
SiO <sub>2</sub>	15.5	54.9	0.2	nd	nd	29.4	nd
TiO <sub>2</sub>	19.1	58.6	nd	16.1	3.5	2.7	nd
TiSi <sub>2</sub>	18.2	50.2	nd	6.4	nd	25.2	nd

nd=element not detected; atomic % < 0.2%.

**Table 5.** XPS Results for Inorganic Plasma-Sprayed Coatings  
(atomic percent)

Compound	C 1s	O 1s	Na 1s	Ti 2p	Al 2p	Si 2p	P 2p*/Mg 2p#
Al <sub>2</sub> O <sub>3</sub>	21.6	48.2	2.9	nd	27.3	nd	nd
AlPO <sub>4</sub> **	24.4	49.6	1.7	nd	2.9	11.1	9.6*
MgO	32.4	48.1	nd	nd	nd	1.7	17.8#
SiO <sub>2</sub>	10.0	64.1	nd	nd	nd	25.9	nd
TiO <sub>2</sub>	31.7	49.7	0.7	16.2	nd	1.7	nd
TiSi <sub>2</sub>	12.1	59.4	nd	1.3	nd	27.2	nd

nd=element not detected; atomic % < 0.2%.; \*\* Nitrogen atomic % = 0.7

The XPS data for the inorganic powders and plasma-sprayed specimens (Tables 4 and 5) suggest that the elemental ratios of the principal elements are not stoichiometric, and that many of the sprayed specimens contain elements other than their principal elements. The principal contaminant element was carbon. To determine the chemical state of the non-principal elements, each element's contribution to the overall oxygen concentration was determined and the carbon photopeaks were curve fitted to determine the contribution of carbon-oxygen functionalities. Stoichiometric allocation and chemical speciation of oxygen in combination with other elements was also carried out. From this allocation procedure, each element's contribution to the total oxygen was determined. In some cases the experimentally measured oxygen content was insufficient to account for all of the oxygen containing species (a deficiency); in other cases there was an excess of oxygen. Excess oxygen in these evaluations could be attributed to adsorbed water or to an element being bound to oxygen in ways not included in the assumptions regarding component stoichiometry and composition being used in the analysis. The results presented are reasonable within the limitations of the XPS measurements and the allocation procedure. The functional group allocation results are summarized in **Table 6**. No attempt was made

**Table 6. Allocation of Oxygen Containing Constituents: Plasma-Sprayed Coatings**

<b>Al<sub>2</sub>O<sub>3</sub>:</b> Total % oxygen in sample;	48.2
Aluminum (Al <sub>2</sub> O <sub>3</sub> )	40.9
Carbon (C-O, C=O, O-C=O <sup>*</sup> )	12.1
Sodium (Na <sub>2</sub> O)	1.5
Oxygen deficiency <sup>*</sup>	-6.3
<b>MgO:</b> Total % oxygen in sample;	48.1
Silicon (silicate)	3.4
Carbon (C-O, C=O, O-C=O <sup>*</sup> )	15.5
Magnesium (MgO, MgCO <sub>3</sub> )	17.5
Excess oxygen <sup>#</sup>	1.7
<b>SiO<sub>2</sub>:</b> Total % oxygen in sample;	64.2
Silicon (SiO <sub>2</sub> )	51.8
Carbon (C-O, C=O)	6.2
Excess oxygen	6.2
<b>TiO<sub>2</sub>:</b> Total % oxygen in sample;	49.7
Titanium (TiO <sub>2</sub> )	32.4
Carbon (C-O, C=O, O-C=O <sup>*</sup> )	8.8
Sodium (Na <sub>2</sub> O)	0.4
Silicon (silicate)	3.4
Excess oxygen	4.7
<b>TiSi<sub>2</sub>:</b> Total % oxygen in sample;	59.4
Titanium (titanium silicate)	7.8
Silicon (SiO <sub>2</sub> )	49.2
Carbon (C-O, C=O)	4.3
Oxygen deficiency	-1.9

<sup>\*</sup> Oxygen deficiency means that the total measured percent oxygen in the sample, i.e. 48.2% for Al<sub>2</sub>O<sub>3</sub>, was less than the amount attributed to the various oxygen-containing species. <sup>#</sup> Excess oxygen means that the total measured percent oxygen in the sample, i.e. 48.1% for MgO was greater than the amount attributed to the various oxygen-containing species.

to allocate the oxygen in plasma-sprayed aluminum phosphate since silica was added as a flow agent during aluminum phosphate deposition.

The allocation procedure yielded results that were consistent with the known stoichiometry for plasma-sprayed  $\text{Al}_2\text{O}_3$ ,  $\text{SiO}_2$ , and  $\text{TiO}_2$ . The success of the allocation is likely due to the fact that there were very few contaminants in these plasma-sprayed samples. The plasma-sprayed  $\text{MgO}$  sample contained oxygenated forms of silicon and carbon. Carbonate made up 5.1% of the carbon and was assumed to be bound to magnesium as magnesium carbonate; the remainder of magnesium was assumed to be  $\text{MgO}$ . The small amount of unassignable oxygen (1.7%) is likely within the limits and expectations of the functionality allocation procedure.

The interpretation of the results obtained for the  $\text{TiSi}_2$  plasma-sprayed sample presented a challenge because the titanium concentration was 1.3% and the silicon atomic concentration was 27.2% not 2.6 atomic % as expected for the 1:2 stoichiometric ratio for  $\text{TiSi}_2$ . The chemical states of titanium and silicon for the plasma-sprayed sample are different than the corresponding chemical states for the powder. The titanium 2p region for  $\text{TiSi}_2$  powder, shown in **Figure 13**, exhibited two photopeaks for titanium, the  $\text{Ti } 2p_{3/2}$  peak at 453.3 eV corresponds to titanium metal and the  $\text{Ti } 2p_{3/2}$  peak at 459.1 eV is assigned to  $\text{TiSi}_2$ . Also, the silicon 2p spectra, presented in **Figure 14**, indicated two chemical states in the powder sample. One Si 2p peak at 98.2 eV corresponds to silicide and the Si 2p sample, i.e. 48.1% for  $\text{MgO}$ , was greater than the amount attributed to the various oxygen containing species. peak at 102.5 eV is assigned to silicate. The differences in the spectra for the plasma-sprayed sample and the powder could be attributed to 1) titanium silicate and  $\text{SiO}_2$  in the plasma-sprayed sample, 2)  $\text{TiO}_2$  and  $\text{SiO}_2$  in the plasma-sprayed specimen or 3)  $\text{TiSi}_2$  and  $\text{SiO}_2$  in the plasma-sprayed adherend. The binding energy for the  $\text{Ti } 2p_{3/2}$  photopeak ( $\text{Ti } 2p_{3/2}$ ; BE = 459.7 eV) for the plasma-sprayed sample was not equivalent to that for  $\text{TiO}_2$  ( $\text{Ti } 2p_{3/2}$ ; BE = 458.5 eV) nor for  $\text{TiSi}_2$  ( $\text{Ti } 2p_{3/2}$  BE = 459.3 eV). Only one

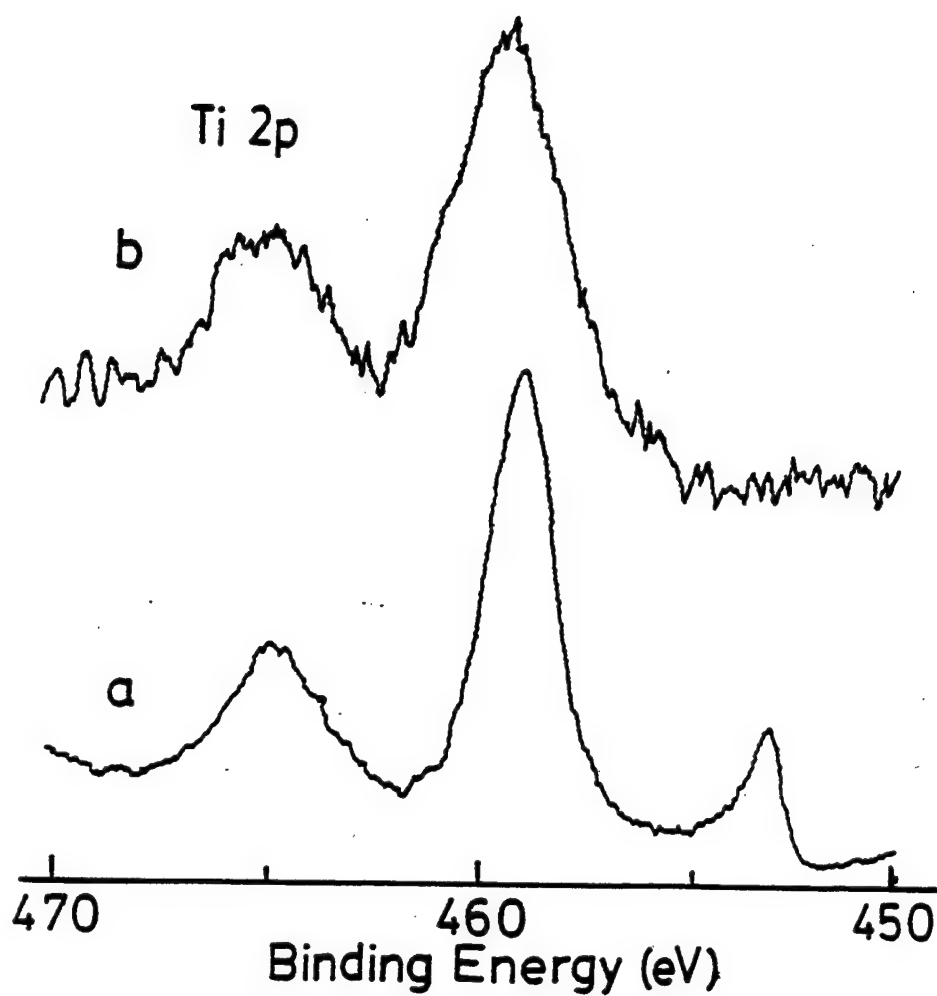


**Figure 13.** Titanium 2p x-ray photoelectron spectra for: a) TiSi<sub>2</sub> powder; b) TiSi<sub>2</sub> powder plasma-sprayed on titanium.

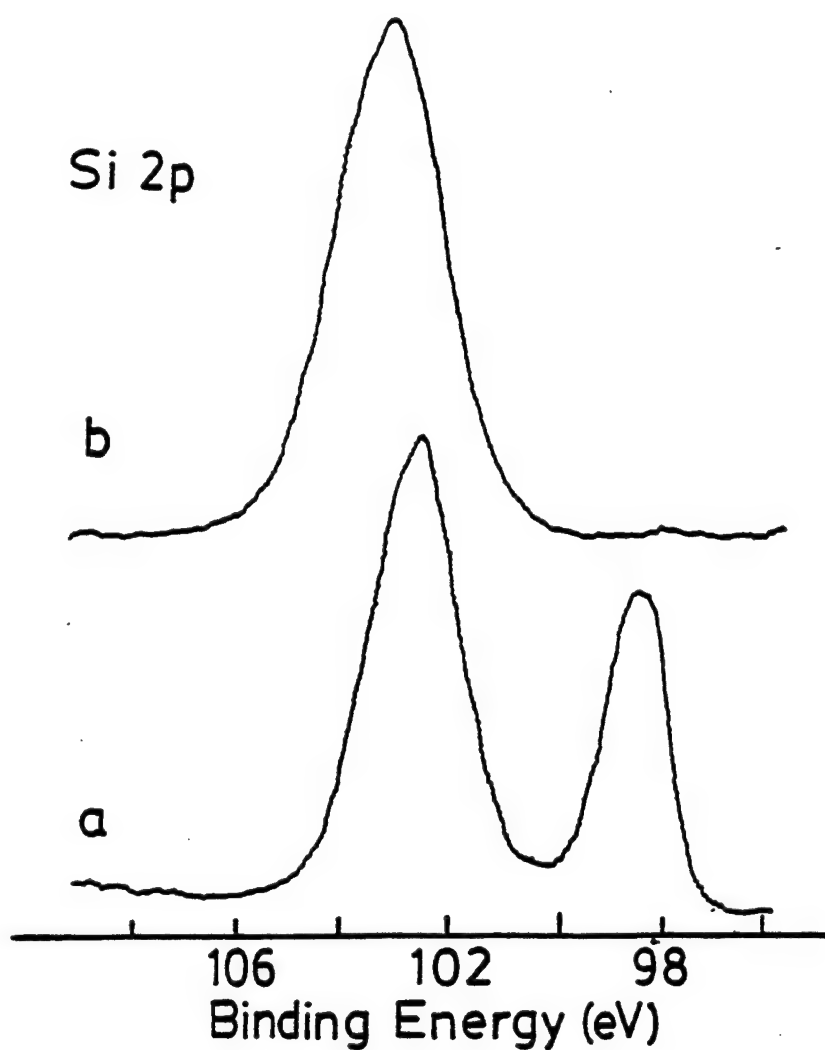


**Figure 14.** Silicon 2p x-ray photoelectron spectra for: a) TiSi<sub>2</sub> powder, b) TiSi<sub>2</sub> powder plasma-prayed on titanium.

silicon 2p photopeak was detected on the plasma-sprayed sample. The single silicon 2p photopeak had a binding energy of 103.2 eV, which corresponds to  $\text{SiO}_2$ . No silicon 2p photopeak was detected in the silicide region. From these considerations it is suggested that a titanium silicate and  $\text{SiO}_2$  were both present on the plasma-sprayed sample. Even though only one silicon 2p photopeak was detected, it is reasoned that titanium silicate and  $\text{SiO}_2$  were present and that the two photopeaks for the two silicon-containing species overlap.



## 5. Plasma-Sprayed Adherends - Durability of Adherends Coated with Inorganic Materials

The durability results, presented as crack length as a function of time, are presented in **Figures 15-18**. Figures 15 and 16 present crack length data for up to 172 hrs of exposure in the environmental cycle for aluminum and titanium samples, respectively. For exposure times of greater than 120 hours (according to cycle B), it was noted that crack length did not change in the period 172 to 3500 hrs. The final crack length data, measured at 3500 hours when the experiments were terminated, are presented in Tables 7 and 8. It is apparent from the results in Figures 15 and 16 that crack growth ended during the second repetition of the environmental cycle, i.e., after approximately 48 hours of exposure to two cycles in the environmental conditions. Crack growth occurred at different rates for samples with different surface preparations under different environmental conditions, as shown in Figures 17 and 18. Examination of the results in Figure 17 for the aluminum samples indicates that, except for the 25- $\text{Al}_2\text{O}_3/\text{Al}$  specimens, crack growth in the cold portion of the cycle is small,  $< 2 \text{ mm}$  (0.08"). Exposure to high relative humidity resulted in marked growth,  $>6 \text{ mm}$  (0.24"), for the 150- $\text{AlPO}_4/\text{Al}$  samples. During the exposure to elevated temperature at atmospheric pressure in air, the PAA/Al and 150- $\text{Al}_2\text{O}_3/\text{Al}$  samples exhibited significant crack growth ( $>6 \text{ mm}$ ; 0.24"). In the hot-vacuum portion of the cycle crack growth of greater than 6 mm (0.24") occurred for the 25- $\text{AlPO}_4/\text{Al}$ , 25- $\text{Al}_2\text{O}_3/\text{Al}$ , and 25- $\text{MgO}/\text{Al}$  specimens. For samples where significant growth was not observed, crack growth of approximately 2 mm (0.08") occurred upon exposure to the various conditions of the cycle.

The changes in crack length for the titanium samples during early exposure in the cycle are given in Figure 18. The 50- $\text{SiO}_2/\text{Ti}$ , 150- $\text{MgO}/\text{Ti}$ , and 150- $\text{TiO}_2/\text{Ti}$  samples exhibited growth greater than 6 mm (0.24") during exposure at  $-20^\circ\text{C}$  ( $-5^\circ\text{F}$ ). The crack for the 25- $\text{MgO}/\text{Ti}$  sample grew more than 6 mm (0.24") in the high relative humidity portion of the test cycle. Other specimens showed incremental growth ( $<2\text{-}3 \text{ mm}$ ; 0.08-0.12") during exposure to each of the environmental conditions.

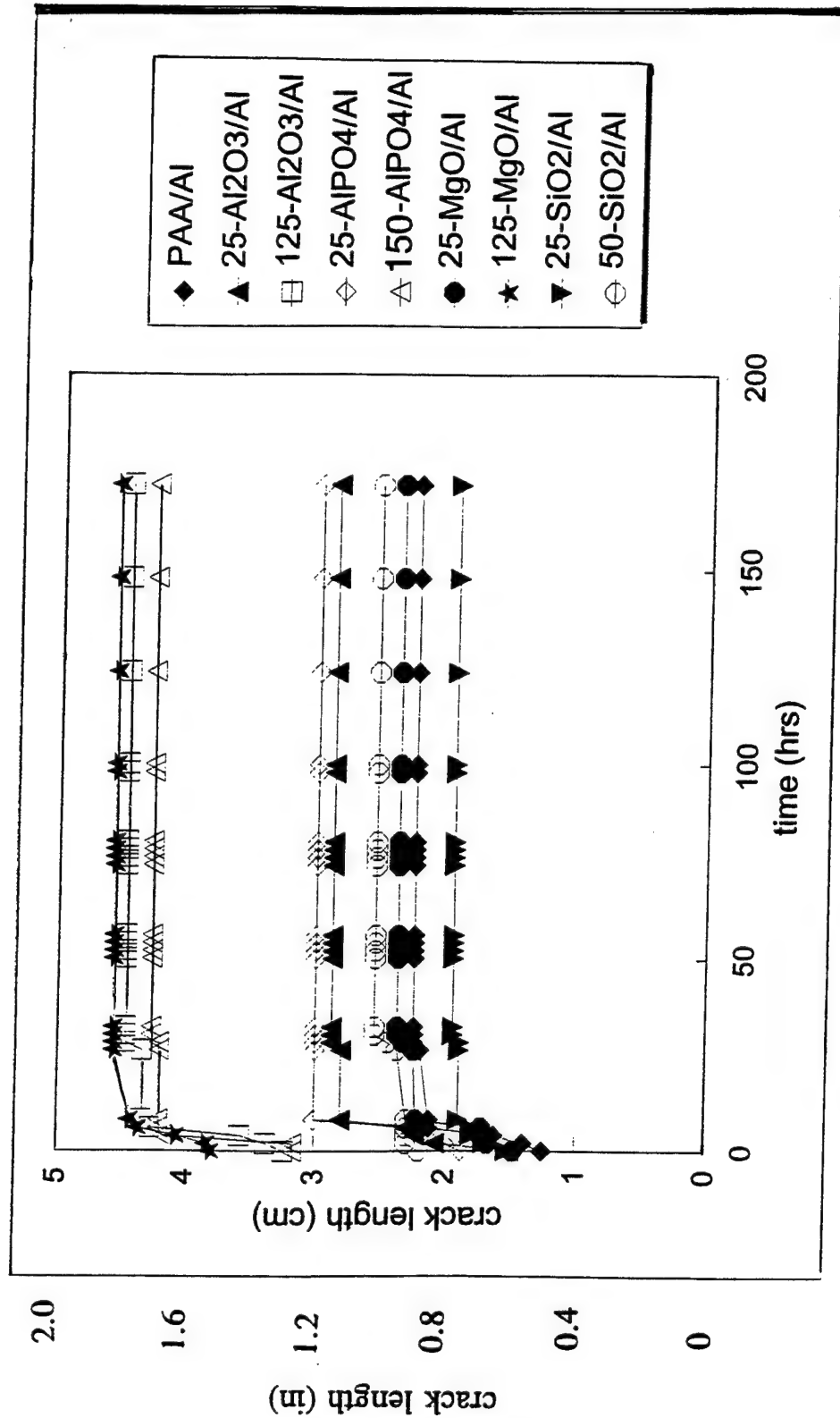


**Figure 15.** Crack Length Results for Plasma-Sprayed Aluminum Adherends Bonded with FM-36 Polyimide Adhesive; Time: 0 to 172 hrs. Total environmental exposure duration 3500 hrs. Crack lengths at 172 hrs. equal to lengths at 3500 hrs.

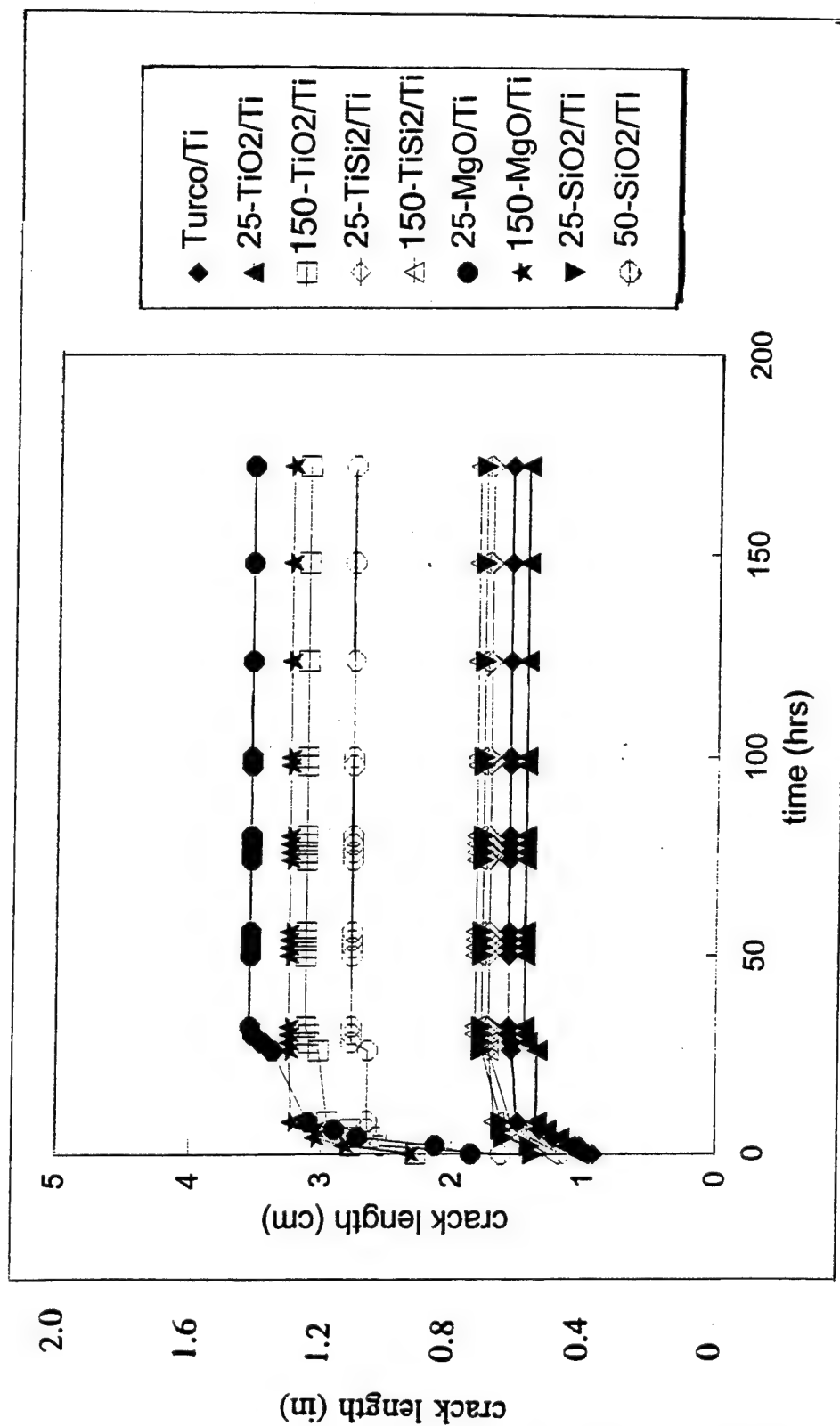


**Figure 16.** Crack Length Results for Plasma-Sprayed Titanium Adherends Bonded with FM-36 Polyimide Adhesive; Time: 0 to 172 hrs. Total environmental exposure duration 3500 hrs. Crack lengths at 172 hrs. equal to lengths at 3500 hrs.

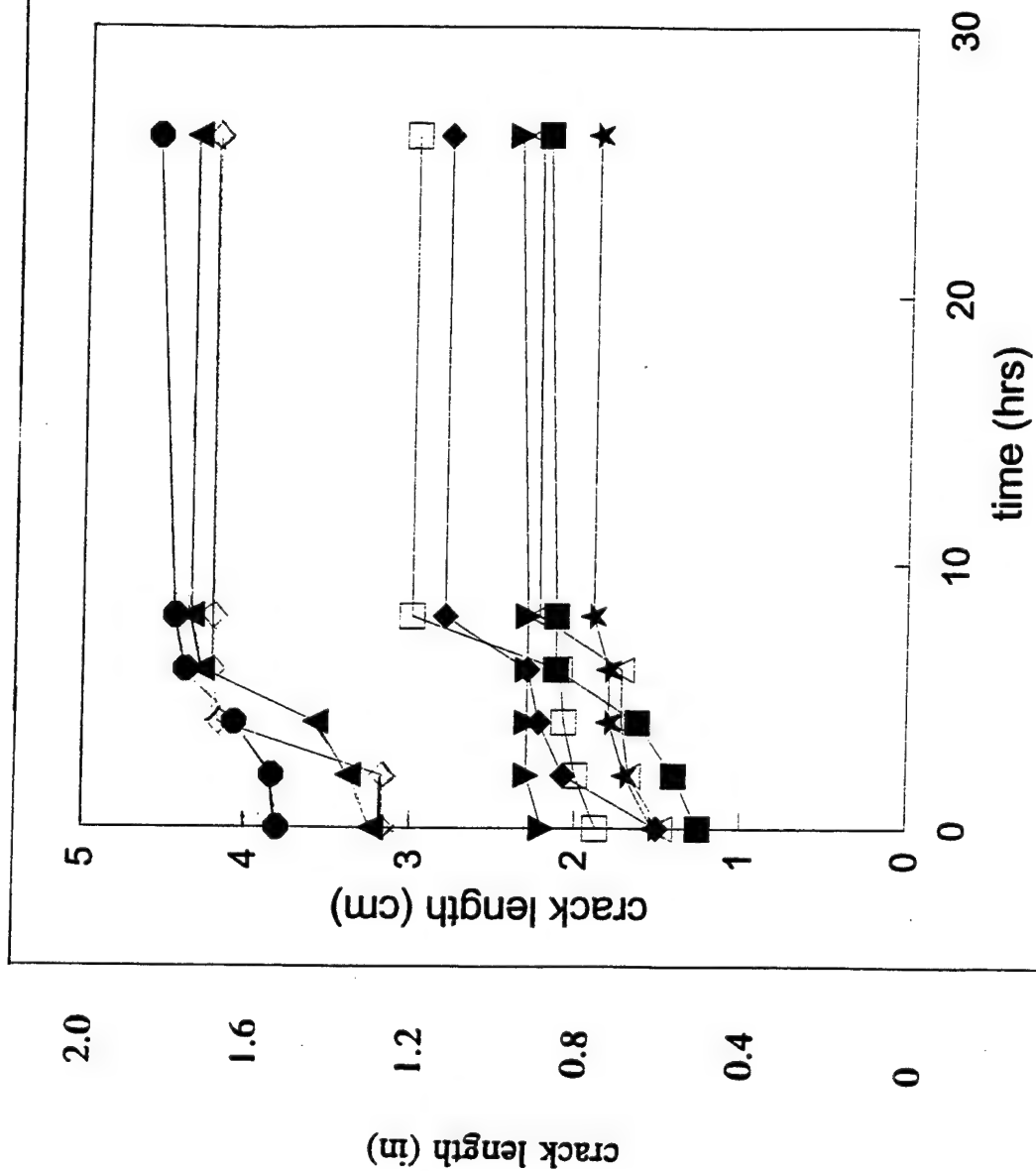


**Figure 17.** Crack Length Results for Plasma-Sprayed Aluminum Adherends Bonded with FM-36 Polyimide Adhesive; Crack length during the first environmental cycle.

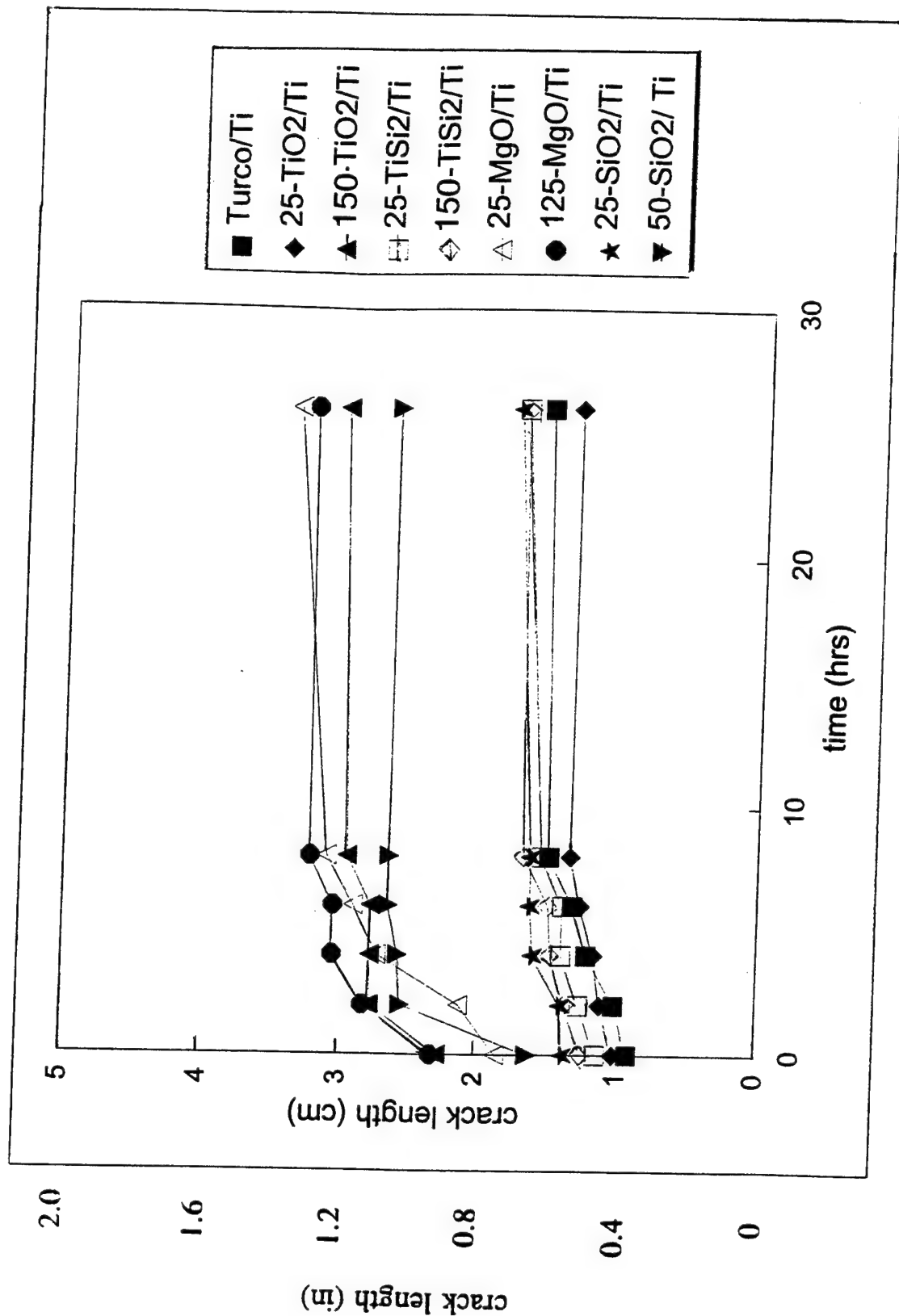


**Figure 18.** Crack Length Results for Plasma-Sprayed Titanium Adherends Bonded with FM-36 Polyimide Adhesive; Crack length during the first environmental cycle.

Returning to a consideration of the general crack growth behavior (Figures 15 and 16), it is apparent for the aluminum adherends that the ultimate crack length is dependent on the surface treatment and that at least two types of general behavior are noted. Crack length values in the range 4.3-4.6 cm (1.7-1.8") are found for the 150-MgO/Al, 150-Al<sub>2</sub>O<sub>3</sub>/Al, and 150-MgO/Al samples. Crack lengths of intermediate and lesser values (<4.0 cm; 1.6") were recorded for all other aluminum samples. Similarly, the crack length is small (<2.0 cm; <0.08") for the 25-TiO<sub>2</sub>/Ti, Turco/Ti, 25-SiO<sub>2</sub>/Ti, 25-TiSi<sub>2</sub>/Ti, and 150-TiSi<sub>2</sub>/Ti specimens. The other titanium samples, 50-SiO<sub>2</sub>/Ti, 150-TiO<sub>2</sub>/Ti, 25-MgO/Ti, and 150-MgO/Ti exhibited crack lengths in the range 2.8-3.6 cm (1.1-1.4"). It is noteworthy that the initial crack lengths for the titanium samples are less than that for the corresponding aluminum specimens. The crack length data indicate a dependence on the coating thickness, in that the specimens with thicker coatings generally showed greater crack growth. The exceptions to this general observation include the 50-SiO<sub>2</sub>/Ti and 150-TiSi<sub>2</sub>/Ti samples. The lower crack length for the 150-TiSi<sub>2</sub>/Ti specimen may be related to the fact that the chemical nature of plasma-sprayed TiSi<sub>2</sub> was found (25) to be a titanium silicate or a mixture of TiO<sub>2</sub> and SiO<sub>2</sub>. It is possible that such a "mixed" chemistry coating could enhance adhesive bonding to the polyimide or inhibit environmental degradation of the bond, and thus improve durability. The findings regarding durability and coating thickness in this study are similar to the results of Pike, et al. for Al<sub>2</sub>O<sub>3</sub> plasma-sprayed on a variety of adherends (23). In recent work, Davis and co-workers (24) reported poor performance, compared to the findings in this study, for aluminum plasma sprayed with alumina and bonded with an epoxy adhesive. It was suggested (24) that primer penetration enhanced the bonding in the current study. However, since no primer was used, it is possible that the porosity of the coating in this work may have allowed penetration of polymer into the plasma sprayed coating, thus enhancing durability. In another study by Clearfield, et al., who plasma-sprayed titanium-6Al-4V on titanium-6Al-4V (7), it was shown that thin plasma-sprayed coatings exhibit failure rates equal to or slightly less than reference standards, such as phosphoric-acid anodized aluminum and Turco-treated titanium.

Also in Davis' study (24) it was reported that titanium alloy plasma-sprayed with titanium-6Al-4V alloy and bonded with an epoxy adhesive exhibited durability performance (static exposure to 90% RH at 60°C; 140°F) that was equivalent to that for chromic acid anodized or Turco-treated titanium alloy. The findings in this study complement the results of the earlier study (24), where in the current work it is demonstrated that titanium-6Al-4V specimens prepared with thin (25  $\mu\text{m}$ ; 0.001") coatings of  $\text{TiO}_2$ ,  $\text{SiO}_2$ , and  $\text{TiSi}_2$ , and thick coatings (150  $\mu\text{m}$ ; 0.006") of  $\text{TiSi}_2$  show excellent bond durability for titanium alloy bonded with a polyimide adhesive.

Exposure of adhesively bonded plasma-sprayed wedge specimens to an environmental cycle resulted in a variety of failure modes and durability behavior. The durability results are summarized in **Tables 7 and 8** for aluminum and titanium adherends, respectively, and are presented in terms of crack length (arrest values) at the end of 3500 hrs in the environmental cycle, and the failure mode induced during environmental exposure. The failure modes were determined either visually or by XPS/SEM surface analysis. The XPS analysis results for the failure surfaces for the 25- $\text{Al}_2\text{O}_3/\text{Al}$  and 150- $\text{Al}_2\text{O}_3/\text{Al}$  specimens are given in **Table 9**.

**Table 7. Failure Processes for Plasma Sprayed Adherends: Aluminum Bonded with FM-36 Polyimide Adhesive**

thickness-coat/adherend	arrest crack		failure mode (XPS)
	length (cm)	(in)	environmental exposure
PAA/Al	2.3	0.91	cohesive
25-Al <sub>2</sub> O <sub>3</sub> /Al	2.9	1.1	cohesive
150-Al <sub>2</sub> O <sub>3</sub> /Al	4.5	1.8	in the coating
25-MgO/Al	2.4	0.94	cohesive
150-MgO/Al	4.6	1.8	mixed mode (coating/cohesive)
25-SiO <sub>2</sub> /Al	2.0	0.79	cohesive
50-SiO <sub>2</sub> /Al	2.6	1.0	cohesive
25-AlPO <sub>4</sub> /Al	3.0	1.2	mixed mode (coating/cohesive)
150-AlPO <sub>4</sub> /Al	4.3	1.7	mixed mode (coating/cohesive)

**Table 8. Failure Processes for Plasma Sprayed Adherends: Titanium Bonded with FM-36 Polyimide Adhesive**

thickness-coat/adherend	arrest crack		failure mode (XPS)
	length (cm)	(in)	environmental exposure
Turco/Ti	1.6	0.63	cohesive
25-TiO <sub>2</sub> /Ti	1.5	0.59	cohesive
150-TiO <sub>2</sub> /Ti	3.1	1.2	coating/metal interface
25-MgO/Ti	3.6	1.4	cohesive
150-MgO/Ti	3.3	1.3	coating/metal interface
25-SiO <sub>2</sub> /Ti	1.8	0.71	cohesive
50-SiO <sub>2</sub> /Ti	2.8	1.1	cohesive
25-TiSi <sub>2</sub> /Ti	1.7	0.67	mixed mode (coating/cohesive)
150-TiSi <sub>2</sub> /Ti	1.8	0.71	mixed mode (coating/cohesive)



**Table 9.** Surface Analysis Results for Al<sub>2</sub>O<sub>3</sub>/Al Plasma-Sprayed Specimens and Failure Surfaces.

element/specimen	Al <sub>2</sub> O <sub>3</sub> /Al	150-Al <sub>2</sub> O <sub>3</sub> /Al		25-Al <sub>2</sub> O <sub>3</sub> /Al	
	non-bonded	adh*	met*	adh	met
C	21.6	21.8	15.0	66.9	69.0
O	48.2	50.5	58.2	22.5	21.8
Al	27.3	24.8	26.3	2.4	1.8
N	<0.2	0.9	0.5	5.3	5.7
Si	<0.2	<0.2	<0.2	3.0	1.8
Na	2.9	<0.2	<0.2	<0.2	<0.2

\* adh: adhesive-side failure surface

met: metal-side failure surface

The results for the two 150-Al<sub>2</sub>O<sub>3</sub>/Al failure surfaces are equivalent and suggest that failure occurs in the coating. For the 150-Al<sub>2</sub>O<sub>3</sub>/Al failure surface the carbon concentrations are in the range 15-22%, the oxygen concentrations are 50-58%, and the aluminum content is approximately 25%. Nitrogen and silicon are present at low concentrations or were not detected. That failure in the coating occurred is supported by the result that the surface chemistries for the two 150-Al<sub>2</sub>O<sub>3</sub>/Al failure surfaces are the same within experimental error, and are similar to the results for a non-bonded plasma-sprayed Al<sub>2</sub>O<sub>3</sub>/Al adherend (25). The respective analysis results for the failure surfaces for the 25-Al<sub>2</sub>O<sub>3</sub>/Al specimens are also equivalent and are consistent with cohesive failure. The carbon, oxygen, and nitrogen concentrations are indicative of adhesive. The presence of silicon may arise from filler in the adhesive. The detection of aluminum on the failure surface may indicate a small contribution from a debonding process where failure occurs at the adhesive/alumina coating interface or within the coating. Nevertheless, the dominant failure mode is cohesive.

Surface analysis results for the MgO-coated/aluminum samples and the TiO<sub>2</sub>-coated/titanium specimens indicated the same failure behavior as for the Al<sub>2</sub>O<sub>3</sub>-coated/aluminum materials. In general the failure modes for the wedge specimens were independent of the type of adherend. The results indicate that the wedge specimens with a thin plasma-sprayed coating (25 μm; 0.001") failed cohesively and that samples with a thick plasma-sprayed coating (150 μm; 0.006") failed within the coating or via mixed mode.

Failure in the AlPO<sub>4</sub>/Al system was unique in that the surface analysis indicates a heterogeneous distribution of components on the failure surface. The XPS results for the analysis of AlPO<sub>4</sub> powder, for the non-bonded plasma-sprayed AlPO<sub>4</sub>/Al surface, and for the metal-side failure surface are presented in **Table 10**.

**Table 10.** Surface Analysis Results for AlPO<sub>4</sub>/Al Plasma-Sprayed Specimens and Failure Surfaces.

element/specimen	AlPO <sub>4</sub> powder	AlPO <sub>4</sub> /Al non-bonded	25-AlPO <sub>4</sub> /Al met*
C	25.3	24.4	30.0
O	47.7	49.6	47.8
Al	11.9	2.9	3.8
N	<0.2	0.7	2.2
Si	<0.2	11.1	1.4
P	11.9	9.6	7.7
Na	3.2	1.7	7.1

\* met: metal-side failure surface

The XPS results for the adhesive-side failure surface were equivalent to the results for the metal-side failure surface. The analysis data for the as received powder are consistent with the expected stoichiometry for AlPO<sub>4</sub>. The powder also contains

carbon and a small amount of sodium as impurities. The plasma-sprayed surface contains silicon at a relatively high concentration. The silicon arises from silica ( $\text{SiO}_2$ ) that was added to enhance the flow of  $\text{AlPO}_4$  in the plasma gun during plasma spraying. The changes in the concentrations of elements on the metal-side failure surface, relative to the values for the plasma-sprayed surface, reveal an increase in carbon, sodium, and nitrogen and a significant decrease in silicon. The concentrations for oxygen, aluminum, and phosphorus are little changed upon comparing the results for the plasma-sprayed and failure surfaces. That the concentrations of constituents associated with the adhesive increase while the coating component concentrations remain relatively unchanged, and that the silicon content decreases dramatically on the failure surface, suggests that failure occurs in a region where polymer and coating components are present. The presence of polymer and coating components on the failure surface indicates that adhesive has likely penetrated the porous structure of the coating and that failure is directed within this coating-adhesive region.

An objective of this study was to examine durability as a function of surface coating chemistry. From the failure data presented in Table 7 for aluminum it is apparent that the thickness of the coating (mechanical properties) appears to play a prominent role in the failure process. Among the different coatings where the acid/base nature is changed;  $\text{SiO}_2$  (acid),  $\text{Al}_2\text{O}_3$ ,  $\text{MgO}$  (base), the crack length and failure modes are similar for the  $25\text{ }\mu\text{m}$  ( $0.001''$ ) coated specimens. Similarly, for the 150- $\text{Al}_2\text{O}_3/\text{Al}$  and 150- $\text{MgO}/\text{Al}$  samples the crack lengths are equivalent and failure occurs in the coating region. The findings for titanium adherends (Table 8) are similar to the results for the aluminum samples, with the exception that both  $\text{MgO}$ -coated adherends exhibit the same crack length but the failure modes are different. The  $\text{TiSi}_2/\text{Ti}$  specimens show excellent durability as indicated by the crack length but mixed mode failure occurs. The type of mixed mode failure is of the type noted for the  $\text{AlPO}_4/\text{Al}$  specimens in that adhesive and coating components were present on both failure surfaces. Such results suggest polymer penetration into the coating and failure in the coating-polymer domain. The durability of the  $\text{TiSi}_2/\text{Ti}$  samples may also be

enhanced by the chemical nature of the coating which was characterized as a titanium silicate or a mixture of  $\text{TiO}_2$  and  $\text{SiO}_2$ . (25). The presence of the silicate, or titania plus silica, may inhibit moisture intrusion into the bond and/or provide a "composite-like" material (silicate plus polymer) whose mechanical properties direct crack propagation away from the adhesive or the adherend/coating interface.

## **6. Plasma-Sprayed Adherends - Durability of Adherends Coated with Polymeric Materials**

The results of the durability experiments are summarized in **Figures 19 and 20**. In Figure 19 the crack growth data for aluminum and titanium specimens bonded with the epoxy adhesive are given. In Figure 20 the corresponding crack growth results for specimens bonded with the polyimide adhesive are illustrated. Although the results in Figures 19 and 20 present data for up to 172 hrs, the exposure experiments were carried out for 3500 hrs. No change in crack length was found during the time period 172 to 3500 hrs. The initial (init.) and final, arrest (fin.) crack lengths, and mode of failure produced during environmental exposure are summarized in **Table 11** for aluminum and in **Table 12** for titanium-6Al-4V samples.

### **6.1 Epoxy adhesive**

The findings presented in Figure 19 for specimens bonded with the epoxy adhesive reveal that the respective final crack lengths are similar for aluminum or titanium coated with plasma-sprayed epoxy, polyester, and bismaleimide-TPI. The arrest crack lengths for the comparable pairs of samples are: epoxy/Al and epoxy/Ti, 6.7 (2.6") and 7.2 cm (2.8"), respectively; polyester/Al and polyester/Ti, 4.7 (1.8") and 4.5 cm (1.8"), respectively; and B-TPI/Al and B-TPI/Ti, 3.2 (1.3") and 3.1 cm (1.2"), respectively. Furthermore, when comparing different coatings among the same adherends, the final crack lengths vary in the manner; epoxy > polyester > bismaleimide-TPI. The respective final crack lengths for the bismaleimide-cyanate ester-coated aluminum and titanium are not equivalent; the crack length for B-CE/Al is greater than that for B-CE/Ti. When the performance of the plasma-sprayed aluminum samples is compared with that for PAA prepared aluminum, the specimens prepared with B-CE and B-TPI coatings exhibited comparable durability. Comparable durability is recognized when the respective crack lengths are equivalent to within 1 cm. The

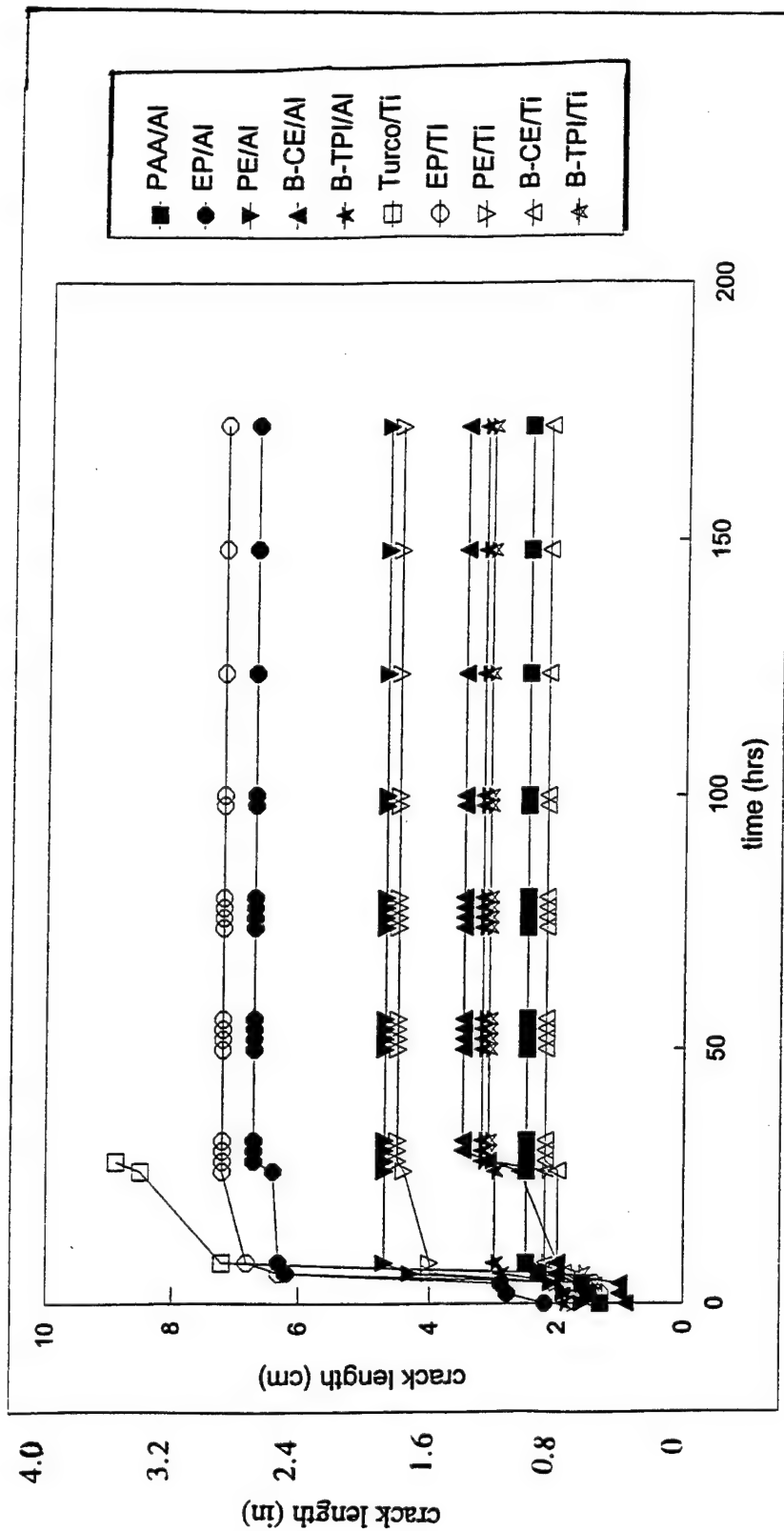
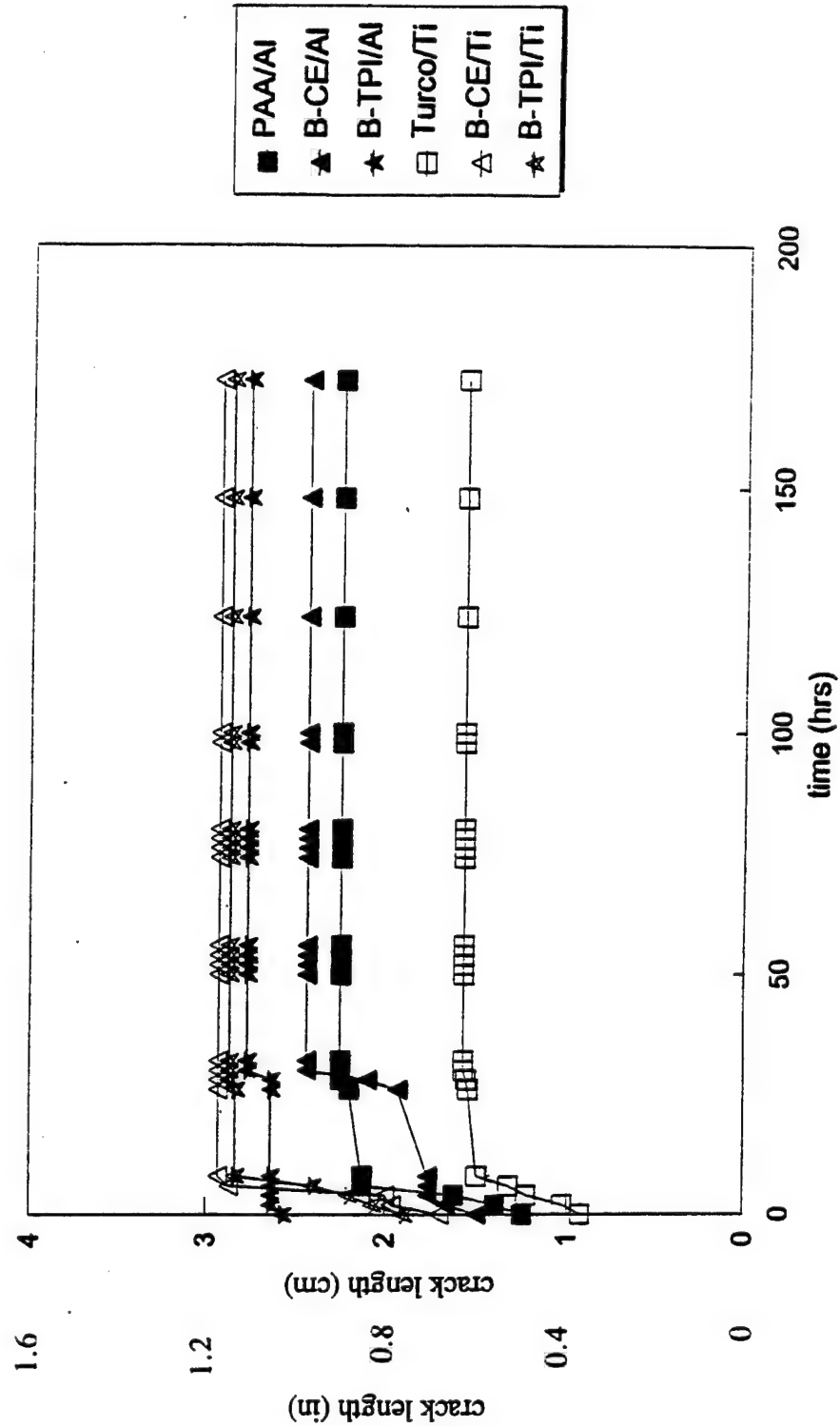


Figure 19. Wedge Specimen Durability: Crack length vs. time of environmental exposure for plasma-sprayed aluminum and titanium bonded with an epoxy adhesive (AF-191).



**Figure 20.** Wedge Specimen Durability: Crack length vs. time of environmental exposure for plasma-sprayed aluminum and titanium bonded with a polyimide adhesive (FM-36).

**Table 11.** Initial and Arrest Crack Length Values and Failure Modes for Plasma-Sprayed Aluminum Adherends. (Crack lengths in cm. and in.)

<u>Aluminum</u>							
coating <sup>1</sup>	epoxy						mode
	init.		fin.		$\Delta^2$		
	cm.	(in.)	cm.	(in.)	cm.	(in.)	
E	2.2	0.87	6.7	2.6	4.5	1.8	mixed <sup>3</sup>
PE	1.6	0.63	4.7	1.9	3.1	1.2	mixed
B-CE	0.9	0.35	3.5	1.4	2.4	0.94	mixed
B-TPI	1.9	0.75	3.2	1.3	1.3	0.51	cohes. <sup>4</sup>
PAA	1.3	0.51	2.5	1.0	1.2	0.47	cohes.
coating <sup>1</sup>	polyimide						mode
	init.		fin.		$\Delta$		
	cm.	(in.)	cm.	(in.)	cm.	(in.)	
E	None <sup>5</sup>						
PE	None						
B-CE	1.5	0.59	2.4	0.94	0.9	0.35	cohes.
B-TPI	2.5	1.0	2.8	1.1	0.3	0.12	cohes.
PAA	1.3	0.84	2.3	0.91	1.0	0.39	cohes.

1. coating: E=epoxy; PE=polyester; B-CE= bismaleimide-cyanate ester;  
B-TPI= bismaleimide LaRC TPI-1500; PAA, phosphoric acid anodized; Turco,  
Turco 5578 treatment.

2.  $\Delta$ : crack extension; final crack length minus initial crack length (cm; in)).

3. mixed: failure at the adhesive-coating and the coating-adherend interface.

4. cohes.: cohesive failure; at the scrim cloth - adhesive interface, or within the  
adhesive.

5. None: No samples prepared.



**Table 12.** Initial and Arrest Crack Length Values and Failure Modes for Plasma-Sprayed Titanium-6Al-4V Adherends. (Crack lengths in cm. and in.)

<u>Titanium-6Al-4V</u>							
coating <sup>1</sup>	epoxy						mode
	init.		fin.		$\Delta^2$		
	cm.	(in.)	cm.	(in.)	cm.	(in.)	
E	1.3	0.84	7.2	2.3	5.9	2.3	mixed <sup>3</sup>
PE	1.7	0.67	4.5	1.8	2.8	1.1	mixed
B-CE	1.4	0.55	2.2	0.87	0.8	0.31	cohes. <sup>4</sup>
B-TPI	1.4	0.55	3.1	1.2	1.7	0.67	cohes.
Turco	1.3	0.51	7.3	2.9	6.0	2.4	mixed
coating <sup>1</sup>	polyimide						mode
	init.		fin.		$\Delta^2$		
	cm.	(in.)	cm.	(in.)	cm.	(in.)	
E	None <sup>5</sup>						
PE	None						
B-CE	1.7	0.67	2.9	1.1	1.2	0.47	cohes.
B-TPI	1.9	0.75	2.9	1.1	1.0	2.5	cohes.
Turco	0.9	0.35	1.6	0.63	0.7	0.28	cohes.

1. coating: E=epoxy; PE=polyester; B-CE= bismaleimide-cyanate ester; B-TPI= bismaleimide LaRC TPI-1500; PAA, phosphoric acid anodized; Turco, Turco 5578 treatment.

2.  $\Delta$ : crack extension; final crack length minus initial crack length (cm; in)).

3. mixed: failure at the adhesive-coating and the coating-adherend interface.

4. cohes.: cohesive failure; at the scrim cloth - adhesive interface, or within the adhesive.

5. None: No samples prepared.

durabilities of polyester- and epoxy-coated aluminum are regarded as less than that for PAA/Al due to the greater extent of crack growth; PAA/Al, 2.5 cm (1.0"); PE/Al, 4.7 cm (1.9"), and E/Al, 6.7 cm (2.6"). It is also noteworthy that the failure mode correlates with the extent of crack growth for the PAA/Al, PE/Al, and E/Al specimens. Cohesive failure was noted for PAA/Al samples whereas mixed mode failure was found for PE/Al and E/Al adherends. Based on crack growth, the performance of B-CE/Al is similar to that for PAA/Al. However, it could be argued that the performance of the CE/Al should be regarded as inferior when compared to PAA/Al due to the fact that mixed mode failure was observed for B-CE/Al. Alternatively, one could consider crack extension,  $\Delta$ , the difference in final and initial crack lengths. Crack growth extension indicates that the performance for B-TPI/Al is equivalent to that for PAA/Al and that the  $\Delta$  values vary in the manner E/Al > PE/Al > B-CE/Al > B-TPI/Al  $\approx$  PAA/Al. Based on crack length, crack extension, and the mode of failure results, it is reasoned that the durability of B-TPI/Al is equivalent to that for PAA/Al while B-CE/Al exhibits marginal durability. Upon considering crack growth and crack extension, the performance for epoxy- and polyester-coated aluminum is regarded as inferior and unacceptable.

The durability performance for coated titanium bonded with epoxy reveals a situation similar to that for aluminum. Although the Turco treated specimens failed completely, the performance for B-CE/Ti and B-TPI/Ti specimens exhibited excellent performance. The arrest crack lengths and the extent of crack growth are low and similar to the values recorded for aluminum adherends. The failure modes for B-CE/Ti and B-TPI/Ti were cohesive. Cohesive failure was easily identified because supporting scrim cloth was visible on all failure surfaces and confirmed that debonding occurred at the scrim cloth-adhesive interface. The crack lengths and extent of crack growth for the PE/Ti and E/Ti specimens were significantly greater than for the B-CE/Ti and B-TPI/Ti samples. In addition, the PE/Ti and E/Ti specimens failed via a mixed mode process. Thus for titanium bonded with epoxy adhesive, the cyanate ester- and the TPI-coated samples showed durability that is regarded as acceptable.

## 6.2 Polyimide adhesive

Aluminum and titanium, plasma-sprayed with bismaleimide-cyanate ester and bismaleimide-TPI mixtures were studied. Specimens were not prepared with epoxy or polyester coatings for bonding with the polyimide adhesive. The results in Tables 11 and 12 and in Figure 20 indicate that the crack lengths are approximately the same as for comparably prepared specimens that were bonded with the epoxy adhesive. All specimens bonded with the polyimide adhesive failed cohesively. As was the case for epoxy-bonded samples, scrim cloth was evident on all failure surfaces; indicating cohesive failure. One could argue that if adhesive and the plasma-sprayed polymer intermix during the curing process, that a more accurate statement would be that failure occurred in the adhesive-plasma-sprayed coating region. Because of the difficulty of interpreting surface analysis data for these failure surfaces, it is not possible to determine unequivocally whether adhesive-coating mixing occurred. On the other hand, it is likely that such mixing could have occurred when it is recognized that the topographical features of the plasma-sprayed B-TPI coating showed nodular, porous features (25) which would permit adhesive penetration into the coating. By contrast the topography for the B-CE/Ti sample was smooth and featureless (25), so intermixing and movement of adhesive into voids in the coating would be unlikely. The important observation is that failure did not occur at the plasma-sprayed coating/adherend interface.

The performance for B-TPI on aluminum and titanium is similar, while the crack length for B-CE/Al is slightly less than that for B-CE/Ti. In fact, the performance for B-CE/Ti and B-TPI/Ti is, within experimental error, indistinguishable. The performance for Turco-treated titanium is better than that for the polymer coated specimens. The arrest crack length, 1.6 cm (0.63"), is less than that for either B-CE/Ti or B-TPI/Ti, both 2.9 cm (1.1"). Although the failure mode for all titanium specimens was cohesive, the extent of crack growth varies in the manner B-CE/Ti > B-TPI/Ti > Turco/Ti. Nevertheless, the important results of the durability tests is that failure occurs cohesively indicating that

the plasma sprayed coating-adherend interaction is significant and that the coating is not degraded in the extensive environmental cycle.

In comparing the performance of the polymer coated-Al specimens with anodized aluminum it appears that equivalent performance is observed. The crack lengths, crack extensions, and failure modes (See Table 11) are all equivalent. Thus the durability of aluminum plasma-sprayed with polymeric components is comparable to that for anodized aluminum.

Although the material systems and the environmental conditions for the durability experiments were not the same, it is of interest to compare the present results with the findings of Davis, et al. (24) where plasma-sprayed polymeric coatings were studied. Davis and coworkers (24) investigated crack growth at 95% RH at 60°C (140°F) for epoxy-bonded plasma-sprayed aluminum. The polymeric coatings included a polyester, PEEK, and mixtures of an aluminum-silicon alloy/polyester, aluminum/polyester, and aluminum/PEEK. For unprimed specimens bonded with FM-123 epoxy adhesive, the wedge specimen crack data for 60Al-Si/40polyester were: crack length 6.5 cm (2.6") and crack extension 2.3 cm (0.91"); while for PEEK (180  $\mu$ m thickness; 0.0072") the results were crack length 8.7 cm (3.4") and crack extension 4.2 cm (1.7"). Under dry or wet exposure conditions, failure for the 60Al-Si/40polyester specimen occurred within the coating. Thus the debonding results in the current study for epoxy- and polyester-coated specimens are similar to those in Davis and associates' work (24). Considering the reproducibility of wedge data among different laboratories, and recognizing that the exposure conditions are dissimilar, and that the polyester coatings are somewhat different (pure polyester in this work and a mixture in the report of Davis, et al. (24)), it is reasonable to suggest that the performance of the polyester-based coatings prepared in the two studies is similar.

In evaluating the reported performance for plasma-sprayed polyester-containing specimens bonded with the FM-300 epoxy adhesive, it is noted that performance is excellent for a 50  $\mu$ m (0.002") coating of 60Al-Si/40 polyester on aluminum and that performance degraded as the amount of alloy in the mixture was

reduced. For specimens prepared with polyester at different thicknesses (50  $\mu\text{m}$  (0.002") and 150  $\mu\text{m}$  (0.006"), Davis, et al. (24)) the initial and final crack lengths were greater than those found in this study. In addition failure occurred at the coating interface (24) whereas failure in the current study was mixed mode. Such differences may be the result of different application conditions, dissimilar environmental exposure conditions, or inherent differences in coating performance. From a comparison of the two investigations, it is apparent that plasma-sprayed polymeric coatings on aluminum exhibit excellent durability performance when tested under static (24) or cyclical environmental conditions (this study). A complete understanding of the mechanism(s) or process(es) by which excellent durability is achieved requires additional study of the chemical and physical nature of plasma-sprayed coatings.

## 7. Durability Investigation of Butt-Torsion Specimens

In this part of the investigation the effect of various load levels and environmental exposure on the torsional durability and failure modes of adhesive joints was examined. Initial testing of titanium and aluminum butt-torsion samples was carried out to determine the ultimate torque failure. The titanium surface was prepared using the Turco 5578 process and aluminum was anodized in phosphoric acid and primed with Scotchweld primer as noted in the experimental section. Samples were tested at room temperature and the results are summarized below in **Table 13**. The failed specimens were examined visually to determine the failure mode and this observation is stated in the table.

**Table 13.** Butt-torsion Test Results - Initial Determination of Failure Torque (in-lbs torque).

Epoxy Adhesive: 3M AF-191

Titanium: 40

cohesive

Aluminum: 29

mixed mode; principally cohesive

Polyimide adhesive: AC FM-36

Titanium: 97

cohesive

Aluminum: 51

mixed mode; principally cohesive

It is apparent that the failure and the mode of failure are determined by the nature of the adhesive and by the surface preparation. There is a general pattern to the results in that the failure torque for the epoxy-bonded samples is approximately one-half of that needed to induce failure in the polyimide bonded samples. It is also apparent that the surface preparation procedures are appropriate so that failure is principally via cohesive rather than adhesive (interfacial) failure.

In order to determine the effect of increased loads and to obtain an idea of the magnitude of torque that is optimal for torsional durability studies, three types of

aluminum/epoxy adhesive joints, each with a different surface treatment, were tested at different levels of torque in a hot humid environment. The joints consisted of Al-2024T bolt adherends bonded with an unsupported structural epoxy adhesive film, AF-191 at 0.05 weight from 3M. The three surface treatments for the aluminum were: phosphoric acid anodization, P2 etch, and vinyl phosphonic acid. The joints were loaded at 0, 20, 40, 60 and 80 percent of failure torque values and placed in a humidity chamber at 66°C (150°F) and 70 percent relative humidity until failure. Upon failure, the failure times were recorded and the failure surfaces were analyzed by x-ray photoelectron spectroscopy (XPS) and scanning electron microscopy (SEM).

### 7.1 Load Level and Environmental Exposure

Originally, a torque of 0%, 20%, 30%, and 40% of the average failure torque for a specimen was exerted on bolts of each type of surface treatment. These values of torque were chosen because an adhesive joint is typically design to hold no more than 40% of its failure load. When loaded, the joints were placed into a humidity chamber at 70% relative humidity and 66°C (150°F). Samples that did not fail within 1582 hours of environmental exposure were force failed. The failure surfaces were analyzed with an XPS and SEM to determine failure mode. The number of days to failure, or failure torques, and the failure modes are listed in **Tables 14, 15, and 16**. Because very few of these samples failed within several weeks and because laboratory durability tests are generally accelerated by exposing samples to conditions harsher than those in service, higher percents of the ultimate torque were exerted on new samples. A 60% torque was placed on anodized and P2 etched specimens and an 80% load was placed on anodized samples. These failure results are also listed in **Tables 14, 15, and 16**.

Some additional samples of the three surface treatments without primer were tested at 40% load. The main reason for testing unprimed bolts was to determine if the primer played a role in the formation of bubbles in the adhesive. The results of the

**Table 14: Anodization Failure Results**

Load	Time to Failure or Failure Torque	Failure Mode or Location
Failure Torque (FT)	13.1 in-lbs (12.4 13.1 14.5)	cohesive
0% FT	30.5 in-lbs 20.9 in-lbs 6.5 in-lbs	adhesive/primer interface adhesive/primer interface adhesive/primer interface
20% FT	13.5 in-lbs 26.1 in-lbs 28.0 in-lbs 30.0 in-lbs	adhesive/primer interface adhesive/primer interface adhesive/primer interface adhesive/primer interface
40% FT	21.5 in-lbs 30.0 in-lbs 27.9 in-lbs 22.1 in-lbs	adhesive/primer interface adhesive/primer interface adhesive/primer interface adhesive/primer interface
60% FT	1 hour 1 hour 2 hours	cohesive cohesive cohesive
80% FT	on loading 0.05 hours 1 hour	cohesive cohesive cohesive
40% FT unprimed	10.1 in-lbs 13.7 in-lbs 19.5 in-lbs	adhesive adhesive adhesive



**Table 15: Vinyl Phosphonic Acid Failure Results**

Load	Time to Failure or Failure Torque	Failure Mode or Location
Failure Torque (FT)	18.1 in-lbs (16.8 18.2 19.3)	mixed: cohesive and primer/ phosphonic acid interface
0%	8.2 in-lbs 15.5 in-lbs 18.7 in-lbs 23.1 in-lbs	vinyl phosphonic acid layer " ", cohesive at edge " ", cohesive at edge " ", cohesive at edge
20% FT	17 hours 13 days 10.5 in-lbs 16.0 in-lbs	vinyl phosphonic acid layer vinyl phosphonic acid layer vinyl phosphonic acid layer adhesive,cohesive at edge
40% FT	17 hours 16 days 19.5 in-lbs 21.8 in-lbs	vinyl phosphonic acid layer vinyl phosphonic acid layer " ", cohesive at edge " ", cohesive at edge
40% FT unprimed	on loading on loading on loading	cohesive cohesive cohesive

**Table 16: P2 Etch Failure Results**

Load	Time to Failure or Failure Load	Failure Mode or Location
Failure Torque (FT)	20.2 (18.5 21.9 20.1)	cohesive
0%	20.1 in-lbs 25.3 in-lbs 25.5 in-lbs	adhesive,cohesive at edge adhesive,cohesive at edge adhesive,cohesive at edge
20% FT	16.5 in-lbs 22.5 in-lbs 24.5 in-lbs 24.5 in-lbs	adhesive,cohesive at edge adhesive,cohesive at edge adhesive,cohesive at edge adhesive,cohesive at edge
40% FT	15 days 22.0 in-lbs 24.1 in-lbs 26.0 in-lbs	adhesive,cohesive at edge adhesive,cohesive at edge adhesive,cohesive at edge adhesive,cohesive at edge
60% FT	1 hour 1 hour 2 hours	cohesive cohesive cohesive
40% FT	on loading on loading 1 hour	cohesive cohesive cohesive

unprimed samples are in Tables 14, 15, and 16. The primer had little role on the influence of bubble formation, but does appear to increase joint strength.

### 7.2 Failure Dependence on Load Level

Load level influenced the time to failure, failure torque, and failure mode very little. Samples loaded above 50% of the failure torque failed almost instantly. Most of the samples loaded below 50% load did not fail until force failed. For each surface treatment, the failure loads of those force failed were not significantly different from samples loaded at different percents of the failure torque. For instance, all of the P2 etch samples in Table 15 failed at an average of about 23 in-lbs despite the different load levels.

There is a small variation in bond strength between samples of the same group that is related to the size and number of air pockets. After environmental exposure, the difference is magnified. This is evident in the larger spread of almost 15 in-lbs in the failure torques of the bonds exposed to the environment versus the 4 in-lb spread of the failure torques for bonds that were tested for ultimate strength.

The failure loads of the specimens that were force failed are higher than the failure torques of the specimens that were used to determine the bonds' ultimate strengths. It is most likely that the bond is being strengthened by environmental exposure.

### 7.3 Failure Mode Dependence on Load Level

The failure mode of the specimens was more a function of the amount of environmental exposure than a function of load level. Samples that failed with 2 hours or less of environmental exposure failed cohesively for the most part. The environmental exposure caused failure to occur close to the surface treatment interface as the water changed the chemistry of the adhesive, surface treatments, and adherends.

The anodized specimens loaded above 50% failed cohesively. None of those loaded below 50% failed after 1582 hours, so these were force failed. The force failures occurred at the interface of the primer and the adhesive. The anodized bond that was not primed failed adhesively. There was not a consistent pattern as to how much of the adhesive or where the adhesive was left on each bolt. Sometimes all of the adhesive was on one of the bolts. On other specimens a spot of adhesive surrounded by primer was left on both bolts.

The vinyl phosphonic acid samples that were failed for ultimate strength data failed via a mixture of cohesive failure and failure at the primer/surface treatment interface. The unprimed specimens failed cohesively upon loading to 40% of the failure torque for a primed specimen. The primed vinyl phosphonic acid samples failed in or close to the surface treatment. The designation of adhesive failure mode in the vinyl phosphonic acid results of Table 15, means that failure is between the primer and the surface treatment as determined by the absence of phosphorus on the adhesive side of the failed sample. Those that are listed with failure in the vinyl phosphonic layer had phosphorus present on both sides of the specimen. The difference between adhesive failure and failure in the vinyl phosphonic acid layer is small. Failure mode of samples with either of these designations is most likely crossing over between the surface treatment and the primer. Some of the vinyl phosphonic acid samples that were force failed had a small ring of cohesive failure at the outer radius of the sample. The ring was typically broken in a few areas.

The P2 etched specimens (Table 16) failed cohesively when loaded above 50% of the failure torque and when unprimed. All of those loaded below 50% of the failure torque failed cohesively at the outer radius of the bolts and adhesively at the centers of the bolts. The circular ring of cohesive failure at the outer radius of many of the samples could be formed when initially loaded, in the humidity chamber, or when failed in the Instron. Water usually collects at regions of high stress where it will weaken interfaces. Since the highest stress in the butt joint is at the outer radius, it would be logical to predict that failure at the outer radius would be more adhesive than

failure at the center of the bond. However, the opposite is true. If cohesive failure were to occur during initial loading, the failure regions are easily explained by the outer cohesive failure being caused during loading and the inner adhesive failure being caused by the environment. If the failure occurs in the humidity chamber, the failure may have occurred early in testing or the region of high stress may be acting as a buffer to the flux of water in and out of the bond line. If failure is all occurring during Instron failure, the region of high failure could again be acting as a buffer to the flux of water or the failure could occur first at the outer radius and then at the center a short time later. A ring-like pattern is visible in some of the samples that were failed in the Instron to determine ultimate strengths, so the presence of the ring is most likely a stress related phenomenon more so than a result of the environmental exposure.

As a result of these initial studies on chemically treated specimens, the bonded plasma-sprayed specimens were loaded to 20 percent of the failure load of standard specimens and exposed to a cycle of cold, hot humid, hot dry, hot vacuum, and ambient laboratory environments. Twenty percent load was exerted because joints are typically design to carry 20 to 40 percent of their failure load and the cyclic environment was meant to simulate aircraft service conditions. The results for aluminum and titanium are summarized in **Tables 17 and 18**, respectively. In the tables the time to failure and mode of failure are presented. Time to failure was determined and was used as a measure of specimen durability. Acceptable performance is identified for the samples where not more than half of the specimens failed during the tests, and where cohesive failure was noted. Coating (thickness- $\mu\text{m}$ )/adherend/adhesive component combinations for which acceptable performance has been demonstrated during the tests (up to about 17,000 hrs) included:

Aluminum adherends

25-Al<sub>2</sub>O<sub>3</sub>/Al/epoxy

25-SiO<sub>2</sub>/Al/epoxy

25-Al<sub>2</sub>O<sub>3</sub>/Al/polyimide

25-SiO<sub>2</sub>/Al/polyimide

Titanium adherends

50-SiO<sub>2</sub>/Ti/epoxy

150-MgO/Ti/epoxy

25-TiSi<sub>2</sub>/Ti/epoxy

25-TiO<sub>2</sub>/Ti/polyimide

150-TiO<sub>2</sub>/Ti/polyimide

25-TiSi<sub>2</sub>/Ti/polyimide

25-SiO<sub>2</sub>/Ti/polyimide

TPI/Ti/polyimide

CE/Ti/polyimide

**Table 17. Aluminum Adherend: Plasma-sprayed Butt-torsion Samples**  
epoxy: 701 da (16,824 hr) (exposure time)  
Cycle: Cold, RH, Hot atm, Hot vac, RT

Epoxy		
Coating /Thickness	1 mil #/tot.*	6 mil (SiO <sub>2</sub> : 2 mil)
Al <sub>2</sub> O <sub>3</sub>	0/4	4/4 2,6 hr/hot atm. 1, 295 da/cold cohesive 1, 546 da/ht/vac interface; Al/Al oxide
AlPO <sub>4</sub>	4/4 1, 43 da/hot vac 1,118 da/hot vac 1,141 da/hot vac 1,155 da/hot vac cohesive	4/4 4,6 hr/hot atm. coating
SiO <sub>2</sub>	0/4	4/4 4,6 hr/hot atm. cohesive
MgO	2/4 1,617 da/hot vac 1,656 da/hot vac cohesive	4/4 4,6 hr/hot atm. cohesive
TPI** 3-5 mil coat	2/2 2,6 hr/hot atm. i'face	
PE 3-5 mil coat	4/4 4,6 hr/hot atm. mode-undetermined	
EPX 3-5 mil coat	4/4 4,6 hr/hot atm. adh. gone	
CNEST 3-5 mil coat	2/2 1, 404 da /hot vac. 1, 428 da/RH i'face	
ANODIZE PO <sub>4</sub> <sup>3-</sup>	4/4 4,6 hr/hot atm. mixed mode	

\*number failed/total bonded  
time to failure/environment  
failure mode

\*\*TPI-LaRC-TPI/BMI  
PE-polyester  
EPX-epoxy  
CNEST-cyanate ester/BMI

Table 17 continued. Aluminum Adherend: Plasma-sprayed Butt-torsion Samples  
polyimide: 709 da (17,016 hr)  
Cycle: Cold, RH, Hot atm, Hot vac, RT

Polyimide		
Coating /Thickness	1 mil #/tot.*	6 mil (SiO <sub>2</sub> :2 mil)
Al <sub>2</sub> O <sub>3</sub>	2/4 2,2 da/RH	2/4 1,136 da/hot vac 1,162 da/hot vac coating/adh
AlPO <sub>4</sub>	4/4 1, 4 hr/RH 1,30 da/RT 1,49 da/RH 1,63 da/hot atm. in PO <sub>4</sub> coating	2/4 2, loading coating
SiO <sub>2</sub>	0/4	1/4 1,25 da/hot vac. i'face/coat
MgO	4/4 2, loading 1, 8 hr/hot vac 1,25 da/hot vac Al/MgO i'face	4/4 1, 4 hr/RH 1,26 hr/RH 1, 8 da/RH 1,16 da/RH Al/MgO i'face
TPI** 3-5 mil coat	3/4 1, 326 da/ RH 1, 468 da/ RT 1, 504 da/ RH i'face	
PE 3-5 mil coat	No samples prepared	
EPX 3-5 mil coat	No samples prepared	
CNEST 3-5 mil coat	3/4 1, 6 hr/hot atm. 1, 225 da/hot vac. 1,331 da/RH i'face	
ANODIZE PO <sub>4</sub> <sup>3-</sup>	0/4	

\*number failed/total bonded  
time to failure/environment  
failure mode

\*\*TPI-LaRC-TPI/BMI  
PE-polyester  
EPX-epoxy  
CNEST-cyanate ester/BMI



**Table 18. Titanium Adherend: Plasma-sprayed Butt-torsion Samples**  
 epoxy: 701 da (16,824 hr) (exposure time)  
Cycle: Cold, RH, Hot atm, Hot vac, RT

Epoxy			
Coating/ Thickness	1 mil #/tot.*	6 mil (SiO <sub>2</sub> : 2 mil)	
TiO <sub>2</sub>	4/4 4,6 hr/hot atm. cohesive	0/4	
TiSi <sub>2</sub>	2/4 1,14 da/hot atm. 1,67 da/hot atm. mode undetermined	4/4 4,6 hr/hot atm. mixed	
SiO <sub>2</sub>	3/4 1,248 da/hot vac 1,298 da/hot vac 1,571 da/hot atm cohesive	2/2 2,6 hr/hot atm. cohesive	
MgO	4/4 4,6 hr/hot atm. coating	2/4 1,243 da 1,572 da Lab accident	
TPI** 3-5 mil coat	3/3 2,6 hr/hot atm., undetermined 1,587 da RH, interfacial/adhesive		
PE 3-5 mil coat	4/4 4,6 hr/hot atm. mode undetermined coat & adh removed		
EPX 3-5 mil coat	4/4 4,6 hr/hot atm. mode undetermined coat & adh removed		
CNEST 3-5 mil coat	4/4 4,6 hr/hot atm. mode undetermined		
TURCO 5578	4/4 4,6 hr/hot atm. mode undetermined		

\*number failed/total bonded  
 time to failure/environment  
 failure mode

\*\*TPI-LaRC-TPI/BMI  
 PE-polyester  
 EPX-epoxy  
 CNEST-cyanate ester/BMI

Table 18 continued. Titanium Adherend: Plasma-sprayed Butt-torsion Samples  
epoxy: 701 da (16,824 hr) (exposure time)  
polyimide: 709 da (17,016 hr)  
Cycle: Cold, RH, Hot atm, Hot vac, RT

Polyimide		
Coating/ Thickness	1 mil #/tot.*	6 mil (SiO <sub>2</sub> : 2 mil)
TiO <sub>2</sub>	2/4 2,251 da Lab accident	1/4 1, 509 da/RH cohesive
TiSi <sub>2</sub>	0/4	2/4 1,459 da/hot atm. 1,464 da/lab accid. coat/adh i'face
SiO <sub>2</sub>	0/4	2/4 1,1 da/hot vac. 1,442 da/hot atm. SiO <sub>2</sub> /adh i'face
MgO	4/4 1, 20 da/hot vac 1, 50 da/hot vac 1, 71 da/hot vac 1,191 da/hot vac coating	4/4 1, 20-25 da/hot atm. 2, 30 da/RT 1, 126 da/hot atm. adh/coat i'face
TPI** 3-5 mil coat	1/3 1,207 da/hot vac cohesive	
PE 3-5 mil coat	No samples prepared	
EPX 3-5 mil coat	No samples prepared	
CNEST 3-5 mil coat	2/2 1,171 da/hot vac 1,230 da/hot vac coating and adhesive mixed	
TURCO 5578	0/3	

\*number failed/total bonded  
time to failure/environment  
failure mode

\*\*TPI-LaRC-TPI/BMI  
PE-polyester  
EPX-epoxy  
CNEST-cyanate ester/BMI

## 8. Summary and Conclusions

This characterization study has demonstrated that inorganic-polymeric and organic plasma-sprayed coatings on metal adherends retain their principal chemical characteristics. The physical state of the plasma-sprayed organic-polymeric coatings appears to be dependent on the nature of the polymer used in the plasma spraying process. The surface characterization results indicate that little or no chemical degradation of the polymer takes place under the plasma-spraying conditions used in this study.

The plasma-sprayed inorganic compounds are also little changed as a result of plasma spraying. The coatings exhibit the "splatter-type" features that are characteristic of plasma-sprayed coatings. Using a systematic approach for assigning functional group contributions, the surface chemical composition of the plasma-sprayed coatings appears to be representative of the sprayed compound. In the case of plasma-sprayed MgO however, some carbonate formation was found as a result of the reaction of MgO with carbon dioxide from the air. For plasma-sprayed  $\text{TiSi}_2$  it was suggested that a coating composed of silicon dioxide and a titanium silicate was most consistent with the XPS data.

The principal findings in the study of the durability of adherends plasma-sprayed with inorganic coatings are: 1. The durability of adhesively bonded plasma-sprayed adherends is equivalent to that for adherend surfaces prepared by standard chemical treatments when tested using cyclical environmental exposure conditions. 2. Durability performance is enhanced for thin compared to thick plasma-sprayed coatings. 3. The mechanical, rather than the chemical properties, of the coatings play a significant role in the failure process.

In the investigation of plasma-sprayed polymeric materials the significant durability results are: 1. The durability performance of plasma-sprayed polymeric coatings on aluminum and titanium is comparable to that achieved for aluminum or titanium surfaces prepared using conventional solution treatments. 2. Extensive crack length correlated with mixed mode failure, and small to moderate crack growth

correlated with cohesive failure. 3. Plasma-sprayed mixtures of bismaleimide and polymeric cyanate ester or LaRC-TPI-1500 appear to be viable alternatives to solution pretreatments for the preparation of adherends for adhesive bonding.

## 9. REFERENCES

1. A. J. Kinloch, "Introduction," in Durability of Structural Adhesives, A. J. Kinloch, ed., Applied Science Publishers, London, 1983, p.1.
2. F. M. Fowkes and M. Mostafa, Ind. Eng. Chem. Prod. Res. Dev., **17**, 3 (1978); F. M. Fowkes, Rub. Chem. Tech., **57**, 328 (1984); F. M. Fowkes, D. O. Tischler, J. A. Wolfe, L. A. Lannigan, C. M. Ademu-John, and M. J. Halliwell, J. Polymer Sci., Polymer Chem. Ed., **22**, 547 (1984).
3. L. H. Lee, J. Adhesion Sci. Technol., **5**, 71 (1991).
4. A. J. Kinloch, "Surface Pretreatments", in Adhesion and Adhesives: Science and Technology, Chapman and Hall Ltd., London, 1987, pp. 101-170.
5. H. M. Clearfield, D. K. McNamara, and G. D. Davis, "Surface Preparation of Metals", in Engineered Materials Handbook, Volume 3, Adhesives and Sealants, H. F. Brinson, ed., ASM International, Materials Park, OH, 1990, pp. 259-275.
6. J. S. Ahearn and G. D. Davis, J. Adhesion **28**, 75 (1989).
7. H. M. Clearfield, D. K. Shaffer, S. L. Vandoren, and J. S. Ahearn, J. Adhesion **29**, 81 (1989).
8. J. A. Filbey and J. P. Wightman, J. Adhesion **28**, 1 (1989).
9. J. A. Filbey and J. P. Wightman, J. Adhesion **28**, 23 (1989).
10. R. F. Wegman, Surface Preparation Technology for Adhesive Bonding, Noyes, Publications, Park Ridge, NJ, 1989.
11. H. Herman, Sci. Amer., **259**, 112 (1988).
12. J. H. Zaat, Ann Rev. Mater. Sci., **13**, 9 (1983).
13. E. J. Kubel, Advanced Materials & Processes, **138**, 24 (1990).
14. C. Panagopoulos, A. Koutsomichalis, and H. Badekas, Surf. Coat. Technol., **41**, 343 (1990).
15. E. Pfender, Surf. Coat. Technol., **34**, 1 (1988).
16. T. N. Rhys-Jones, Surf. Coat. Technol., **42**, 1 (1990).

17. T. N. Rhys-Jones and T. P. Cunningham, *Surf. Coat. Technol.*, **42**, 13 (1990).
18. G. N. Heintze and R. McPherson, *Surf. Coat. Technol.*, **34**, 15 (1988).
19. M. K. Hobbs and H. Reiter, *Surf. Coat. Technol.*, **34**, 33 (1988).
20. P. Ostojic and C. C. Berndt, *Surf. Coat. Technol.*, **34**, 43 (1988).
21. D. S. Rickerby, *Surf. Coat. Technol.*, **36**, 541 (1988).
22. Z. Z. Mutasim and R. W. Smith, "Reactive Plasma Spray Forming", Thermal Spray Coatings: Properties, Processes, and Applications: Proceedings from the Fourth National Thermal Spray Conference, May 4-10, 1991, Pittsburgh, PA, 1992, p. 273.
23. R. A. Pike, V. M. Patarini, R. Zatorski, and F. P. Lamm, *Int. J. Adhesion Adhesives* **12**, 227 (1992).
24. G. D. Davis, P. L. Whisnant, D. K. Shaffer, G. B. Groff, and J. D. Venables, *J. Adhesion Sci. Technol.*, **9**, 527 (1995).
25. K. L. Wolfe, K. L. Kimbrough, J. G. Dillard, S. R. Harp, and J. W. Grant, *J. Adhesion*, in press (1995).
26. K. L. Wolfe, S. R. Harp, J. W. Grant, and J. G. Dillard, *J. Adhesion*, (accepted) (1995).
27. J. A. Marceau, Y. Moji, and J. C. McMillan, *Adhesives Age*, **20** (October), 28 (1977); J. Cognard, *J. Adhesion* **20**, 1 (1986).
28. D. Briggs, "Applications of XPS in Polymer Technology", in Practical Surface Analysis by Auger and X-Ray Photoelectron Spectroscopy, D. Briggs and M. P. Seah, Eds., John Wiley, New York, 1983, pp. 359-396.
29. J. G. Dillard, C. Burtoff, and T. Buhler, *J. Adhesion* **26**, 203 (1988).
30. C. D. Wagner, W. M. Riggs, L. E. Davis, J. F. Moulder, Handbook of X-Ray Photoelectron Spectroscopy, G. E. Muilenberg, Ed., Perkin-Elmer, Eden Prairie, MN, 1979.
31. D. Matejka and B. Benko, Plasma Spraying of Metallic and Ceramic Materials, John Wiley, New York, 1989.